NUMERICAL ANALYSIS OF SPATIAL EVOLUTION OF POWER IN AN EDFA UNDER TEMPORAL STEADY STATE

Thesis

Submitted to
School of Engineering
UNIVERSITY OF DAYTON

In partial fulfillment of the requirement for the degree of
Master of Science in Electrical Engineering

By

Mrudula N Garagaparti

School of Engineering
UNIVERSITY OF DAYTON

Dayton, Ohio
May 2006

NUMERICAL ANALYSIS OF SPATIAL EVOLUTION OF POWER IN AN EDFA UNDER TEMPORAL STEADY STATE

APPROVED BY:

Monish R. Chatterjee, Ph.D.
Advisory Committee Chairman
Professor, Department of Electrical Engineering

Partha P. Banerjee, Ph.D.
Committee Member
Professor, Department of Electrical Engineering

Guru Subramanyam, Ph.D.
Committee Member
Associate Professor, Department of Electrical Engineering

Donald L. Moon, Ph.D.
Associate Dean
Graduate Engineering Programs & Research,
School of Engineering

Joseph E. Saliba, Ph.D., P.E.
Dean, School of Engineering

ABSTRACT

NUMERICAL ANALYSIS OF SPATIAL EVOLUTION OF POWER IN AN EDFA UNDER TEMPORAL STEADY STATE

Name: Mrudula N. Garagaparti

Department of Electrical Engineering

University of Dayton, May 2006

Advisor: Dr. Monish. R. Chatterjee

Erbium Doped Fiber Amplifiers (EDFA) have revolutionized long haul fiber optic communication systems. The numerous advantages of erbium amplifier over other amplifiers such as semiconductor laser amplifiers, Raman amplifiers and Brillouin amplifiers have triggered the undertaking of this work. In this work our main objective is to set up power evolution equations for EDFAs and find solutions to these equations. Analysis of power distribution in EDFAs typically proceeds from two sets of equations. The first set of equations depends on the spatial variations of signal, pump and the amplified spontaneous emission (ASE) powers. The second set shows the rate of change with time of population densities of ground and metastable levels in the amplifier. In these equations, power and number densities are coupled together, leading to a highly nonlinear spatial – temporal system. We have used two approaches to solve these equations. In the first approach we have solved power evolution equations numerically. For solving rate equations numerically, we have used the model of a three level laser

system. We have simplified the problem to some extent by assuming that the populations reach temporal steady state (with that we were originally interested in the transient population dynamics). In the second approach we obtained analytic solution to the power equations assuming temporal and spatial steady state of the population densities. We have solved the equations using both approaches, and the numerical graphs for the population densities, signal and ASE power versus distance are plotted. It is found that there is a region (the gain region) where the population, once inverted, remains approximately constant which leads to amplification in the EDFA. Comparing with literature, some physical interpretations of the numerical findings are also summarized in this work.

ACKNOWLEDGEMENTS

I sincerely thank my advisor Dr. Monish Chatterjee for his guidance, inspiration, patience and excellent advising. Without his guidance and support I would never have made this work possible.

I want to thank my committee members Dr. Partha Banerjee and Dr. Guru Subramanyam for their time and patience.

I would like to thank Dr. Malcolm Daniels, Chair of The Department of Electrical and Computer Engineering, for his support.

My special thanks to Arun M Venkataraman for his endless support and guidance in my work.

I am also thankful to my husband Sekhar Kanagala and to all my friends Yoga L. Srinivas Kantamani, Sangameshwar Sonth, Ramakrishna Gudavalli and Divya Kanneganti. I am dedicating this work to my Beloved Parents with whose blessings I accomplish all my endeavors.

TABLE OF CONTENTS

LIST OF FIGURES

LIST OF TABLES

CHAPTER 1

INTRODUCTION

1.1 Background:

The erbium doped fiber amplifier is emerging as a major enabler in the development of world wide fiber optic networks. The emergence of the fiber amplifier foreshadows the invention and development of novel guided wave devices that should play a major role in the continuing increase in transmission capacity and functionality of fiber networks. Currently fiber networks are used predominantly in long distance telephone networks, high density metropolitan areas and in cable television trunk lines. The most vivid illustrations of fiber based transmission systems have been in undersea transcontinental cables [24].

The technique of new light wave amplification *in situ* with vastly improved capacity and cost is based on the recent development of erbium doped fiber amplifiers. Undersea systems were the early beneficiaries, as EDFA repeaters replaced expensive and intrinsically unreliable electronic regenerators. Indeed, early EDFA technology was driven by the submarine system developers who were quick to recognize its advantages soon after the first diode pumped EDFA was demonstrated in 1989 [25]. Terrestrial telecommunications systems have also adopted EDFA technology in order to avoid electronic regeneration. Hybrid fiber/coax cable television networks employ EDFAs to extend the number of homes served. An equally attractive feature of the EDFA is its wide

gain bandwidth product. Along with providing gain at 1550nm in the low loss window of silica fiber it can provide gain over a band that is more than 4000 GHz wide. With available wavelength division multiplexing components, commercial systems transport more than 16 channels on a single fiber; the number is expected to reach 100 within the next decade. Hence, installed systems can be upgraded many fold and new WDM systems can be built inexpensively with much greater capacity.

The erbium amplifier is a three level system as opposed to neodymium, which is a four level system. One significant difference between the two types is that a good deal of more pump power is required to invert the three level system. Hence, neodymium ions were the earliest successful rare earth dopant used in lasers. However, erbium is the more popular choice for fiber dopant because the amplifiers with using this dopant were having high gain and efficiency.

1.2 Historical Development of EDFAs

1.2.1 Origin of optical amplifiers

Optical amplifiers play an exceptionally important role in long haul networks. Prior to the advent of optical amplifiers, the standard way of coping with the attenuation of light signals along a fiber span was to periodically space electronic regenerators along the line [24]. Such regenerators consist of a photodetector to detect the weak incoming light, electronic amplifiers, timing circuitry to maintain the timing of the signals, and a laser along with its driver to launch the signal along the next span. Such regenerators are limited by the speed of their electronic components. Thus even though fiber systems have inherently large transmission capacity and bandwidth due to their optical nature, they are limited by electronic regenerators in the event such regenerators are employed. The cost

and complexity of converting the signal to electronic form in electro optic repeaters, and the associated reduction in speed of operation, created the need for optical amplifiers. Optical amplification is based on stimulated emission. Early laser developers saw amplification via stimulated emission as a step toward building a laser. As opposed to standard electronic repeaters and amplifiers, optical fiber amplifiers are purely optical in nature, and require no high speed circuitry. The signal is not detected and regenerated; rather, it is very simply optically amplified in strength by several orders of magnitude as it traverses the active region of the amplifier *in situ*, without being limited by any electronic bandwidth. The shift from regenerators to amplifiers thus permits a dramatic increase in the capacity and speed of the transmission system, and this feature is being realized in current applications.

The basic concept of a traveling wave optical amplifier was first introduced in 1962 by Geusic and Scovil [1]. Shortly thereafter, an optical fiber amplifier was invented in 1964 by E.Snitzer, then at the American Optical Corporation, who described an unclad neodymium glass fiber amplifier at 1.06 μm. Snitzer later, demonstrated an amplifier in a clad fiber. This work lay dormant for many years thereafter. It emerged as an exceedingly relevant technological innovation after the advent of silica glass fibers for telecommunications. Motivation for developing optical amplifiers prior to the emergence of fiber optic communications was virtually non-existent, except for a few optical amplifiers built to raise pulse powers to very high levels, there was no need for optical amplifiers until the advent of fiber optic communications. One approach was to develop amplifiers from semiconductor lasers used as light sources. Semiconductors have high gain, so suppressing reflection from the end facets of the chip looked attractive.

Stimulated Raman scattering also looked promising because although it required very high pump power, it could be distributed along the entire length of a fiber. Eventually, EDFAs effectively replaced semiconductor optical amplifiers and Raman amplifiers, since the latter suffer serious technical problems.

Snitzer also demonstrated the first erbium doped glass laser [2]. This work represents the earliest fiber laser. Interestingly, rare earth doped lasers in a small diameter crystal fiber form were investigated during the early 70s as potential devices for fiber transmission systems [3]. The crystal fibers had cores as small as 15 μm in diameter, with typical values in the 25 μm to 70 μm range. The crystalline cores were doped with neodymium, surrounded by a fused silica cladding. Lasing of this device was achieved at 1.06 μm. Since commercial fiber-optic transmission systems did not adopt the 1.06 μm wavelength as a signal wavelength, these lasers did not make their way into today's fiber communication systems. The development of low loss single mode fiber lasers was followed by that of fiber amplifiers.

1.2.2 The road to fiber amplifiers

The roots of erbium doped fiber lasers and amplifiers began in 1964 with the first amplification experiments in rare earth doped fiber lasers.

When David Payne of the University of Southampton started down the road to erbium fiber amplifiers, he was looking for fiber lasers or fiber optic sensors. In 1985, he recognized that the next thing to do is to put some rare earths into the fibers. They started with neodymium, the best developed solid state laser dopant. They found that the rare earth ions caused no significant losses at the low doping levels they used [9]. The next step was to make a fiber laser. Payne *et.al* noted that doped fibers could be used to make

an optical amplifier. Solid state lasers had too little gain to provide the 30 dB amplification needed in fiber optic systems. Instead, fiber lasers were experimented with, since power could build with in a resonant cavity. However, fiber lasers were typically several meters in length – long by conventional laser standards.

As indicated before, rare earth elements were already well known as lasers in bulk glass and crystalline hosts. Though the late 1970s and early 1980s, researchers used neodymium, thulium and ytterbium before erbium, noting that the neodymium laser could be tuned across 80nm, while the erbium laser only across 25nm [10].

It turns out that the three level erbium system absorbs strongly around the laser transition at low pump powers and the 1530nm Er^{3+} transition wavelength is also well adapted to propagation in silica fibers. The Southampton group developed the first amplifier in late 1986; the peak gain was 26 dB at 1536 nm in a three meter fiber, pumped at 514.5 nm by a mode locked argon laser [11]. Later, by switching to pumping with a mode locked argon pumped dye laser near 670nm, a peak gain of 28dB was achieved, along with a gain of at least 10 dB between 1530 and 1555nm.

1.2.3 Work on EDFA in 80s

Emmanuel Desurvire and coworkers in 1986 started working on erbium fibers at Bell Laboratories. They built an erbium fiber amplifier, pumping with a continuous wave argon laser at 514.5nm, and developed a theoretical model, optimizing thereby the effective fiber length[28]. The need for a better pump source remained a major issue. Argon lasers used in the laboratory, required 100s of kilowatts of electricity, cooling water and extensive care, often left as assignment to laboratory assistants. Scientists searched the erbium absorption spectrum for pump bands. British Telecom first pumped

an erbium fiber laser at 808nm with a dye laser [12]; The Southampton group later pumped one with a continuous wave 808nm diode laser generating output to 130 microwatts [13]. A high power diode array pump at 800nm increased the laser output. However, pumping with diode arrays at 800nm proved to be inefficient. The excited state absorption was at least as large as ground state absorption for pumping at 810 and 488nm. Excited state absorption was found to be absent at 980nm pumping [14]; however a diode oscillator at 980nm was not available. In 1988 Snitzer attempted operation at 1480nm. A net gain was reported when pumping erbium fiber amplifier with a color center laser at 1490 and 1500nm [5]. Eventually, 1480nm was shown to be the best wavelength choice for the pump. The following year, Desurvire et.al demonstrated 37 dB of gain or a record 2.1 dB per milliwatt of pump power [15]. In late 1989, the Nakazawa group of Japan reached a 46.5 dB gain when pumping an erbium fiber amplifier with 133mW from multiple 1480 nm diode lasers [16]. Diode pumping had compelling advantages for practical fiber amplifiers, and development quickly narrowed to systems pumped at 980nm and 1480nm. The longer wavelength got a headstart because 1480nm lasers were better developed. A decade later, these two wavelengths remain the standard choices today.

Erbium doped fiber amplifiers for traveling wave amplification of 1.5 μm signals were simultaneously developed in 1987 at the University of Southampton and at AT&T Bell Laboratories [11]. A key advance was the recognition that the Er^{3+} ion, with its propitious transition at 1.5 μm was ideally suited as an amplifying medium for modern fiber optic transmission systems at 1.5 μm. The high signal gains obtained with these erbium doped fibers attracted worldwide attention. As the previously mentioned amplifier

demonstrations typically used large frame laser pumps, the final hurdle was to demonstrate an effective erbium doped fiber amplifier pumped by a laser diode or an array. This was achieved in 1989 by Nakazawa and coworkers, after the demonstration by Snitzer *et.al.,* that 1.48 μm was a suitable pump wavelength for erbium amplification in the 1.53 μm to 1.55 μm range[5]. Nakazawa and group were able to use high power 1.48 μm laser diode pumps previously developed for fiber Raman amplifiers[6]. This demonstration opened the way to serious consideration of amplifiers for systems application. Previous work exploring optical amplification with semiconductor amplifiers provided a foundation for understanding signal and noise issues in optically amplified transmission systems [7].

1.3 EDFAs in Transmission Networks:

Starting in 1989, erbium doped fiber amplifiers were the catalyst for an entirely new generation of high capacity undersea and terrestrial fiber optic links and networks. At an optical fiber conference in 1989, Desurvire's group reported that erbium fiber amplifiers could handle signals at multiple wavelengths without crosstalk between channels[17]. By inserting a fiber amplifier after the first 51 km of fiber, researchers at Bellcore stretched the transmission distance to 93.7km, claiming a record for the bit rate distance product for a single amplifier. Bellcore also demonstrated 16 channel wavelength division multiplexing(WDM), using coherent transmission without optical amplifiers and transmitting only 155Mbit/s on each channel [18]. A team from KDD R&D laboratories transmitted 2.4 Gbit/s at four separate wavelengths about 2nm apart through 459 km of fiber using six erbium amplifiers along the route [19]. The first undersea test of erbium doped fiber amplifiers in a fiber optic transmission cable

occurred in 1989[8]. By 1996 erbium doped fiber amplifiers were in commercial use in a number of undersea links increasing the capacity near ten fold over the previous generation of cables.

The first implementation of erbium doped fiber amplifiers has been in long haul systems such as the TAT-12, 13 fiber cable that AT&T and its European partners installed across the Atlantic in 1996 [24]. This cable, the first transoceanic cable to use fiber amplifiers, provides a near ten fold increase in voice and data transmission capacity over the previous transatlantic cable.

With recent advances made throughout the 1990s in a number of optical transmission technologies, be it lasers or novel components such as fiber grating devices or signal processing fiber devices, the optical amplifier offers a solution to the high capacity needs of today's voice and data transmission applications. Commercial erbium fiber amplifiers are finding increasing applications, along with steady improvements in the technology. Today, erbium fiber amplifiers carry signals thousands of kilometers in submarine cables and transmit dozens of channels at 10Gbit/s in commercial land systems [25]. Developers opened up a new erbium fiber window at 1570 to 1620 nm, where gain is lower but still adequate for optical amplifiers. Erbium remains by far the best fiber amplifier dopant.

CHAPTER 2

CHARACTERISTICS OF FIBER BASED OPTICAL AMPLIFIERS

2.1 Optical Amplifiers

As discussed in the previous chapter, the transmission distance of any fiber optic communication system is limited by fiber loss and dispersion. Optical amplifiers in fibers amplify the incident light through stimulated emission, the same mechanism used by lasers. The external pump, either optically or electronically, generates a population inversion in amplification media. Indeed, an optical amplifier is nothing but a laser without feedback, where an amplified photon is a signal photon.

2.1.1 Important Parameters of Optical Amplifiers:

Gain (dB):

An important measure for the amplification ability of an optical amplifier is the optical gain realized when the amplifier is pumped to achieve population inversion. The optical gain in general depends not only on the frequency of the incident signal, but also on the local beam intensity at any point inside the amplifier. In optical amplifiers, gain is defined as the ratio of output to input optical power and is usually expressed in dB through

$$\text{Gain (dB)} = 10 \times \log_{10}[P_{out} / P_{in}] \qquad (2.1)$$

Gain saturation:

When the optical power is too high, the gain coefficient starts to decrease, thus reducing the power of the signal undergoing amplification. This effect is called gain saturation. More precisely, when the optical power P exceeds the saturation optical power $P_{sat,}$ the gain becomes saturated. Gain saturation is an important characteristic to determine the saturated output power.

Saturated output power:

It is the maximum output power P_{out} from an optical amplifier when the optical power within the amplification medium reaches the saturation optical power P_{sat} . The saturated output power P_{out} is usually less than the saturation optical power P_{sat} because the latter is the sum of the input pump power and output power.

Amplified Spontaneous Emission (ASE):

It is the amplified optical power resulting from the spontaneous (i.e., not stimulated by any signal photons) release of photons within the gain spectrum of an EDFA operation due to the random decay of erbium ions from the metastable state to the ground state. A detailed description of the occurrence and effects of ASE is given at a later stage in this chapter.

Noise Figure (dB):

It quantifies the noise performance of an optical amplifier and is defined as the signal-to-noise ratios of the input and output signals:

$$nf = [\mathrm{SNR}]_{in}/[\mathrm{SNR}]_{out} \tag{2.2}$$

It is usually expressed in units of dB, given by

$$NF = 10 \times \log_{10}\{[\mathrm{SNR}]_{in}/[\mathrm{SNR}]_{out}\} \quad (2.3)$$

NF is often referred to as a figure of merit when one is evaluating the noise performance of an optical amplifier. The SNR degradation is quantified through this parameter.

Small Signal Gain (dB):

It is the amplifier gain, when operated in the linear region, where it is essentially independent of the input signal power at a specific signal wavelength and operating conditions (e.g., pump power, temperature …).

2.1.2 Optical Amplifier Applications

Optical amplifiers can serve several purposes in the design of fiber optic communication systems. Four such applications are as follows [23].

Inline amplifiers:

When optical amplifiers are used to replace electronic regenerators as shown in Fig 2.1(a) in long haul systems, they are called in-line amplifiers. They modify a small input signal and boost it for retransmission down the fiber. Controlling the small signal performance and noise added by the EDFA reduces the risk of limiting a system's length due to the noise produced by the amplifying components. Such a replacement can be carried out as long as the system performance is not limited by the cumulative effects of dispersion and spontaneous emission.

Power amplifiers:

Optical amplifiers can also be used to increase the transmitter power by placing them just after the transmitter as shown in Fig 2.1(b). Such amplifiers are called power amplifiers or boosters. This application requires the amplifier to take a large signal input and provide the maximum output level. Small signal response is not as important because the direct transmitter output is usually -10 dBm or higher. The noise added by the amplifier at this point is also not as critical because the incoming signal has a large signal-to-noise ratio (SNR).

Preamplifiers:

In the past, receiver sensitivity of -30 dBm at 622 Mb/s was acceptable; however, currently, the demands require sensitivities of -40 dBm or -45 dBm. This performance can be achieved by placing an optical amplifier prior to the receiver which is shown in the Fig 2.1(c). Boosting the signal at this point presents a much larger signal into the receiver, thus easing the demands of the receiver design. This application requires careful attention to the noise added by the amplifier; the noise added by the amplifier must be minimal to maximize the received SNR.

LAN amplifier:

Another application of optical amplifiers is to use them for compensating distribution losses in local area networks (LANs) [29]. Such amplifiers are called LAN amplifiers and they are depicted in the Fig 2.1(d).

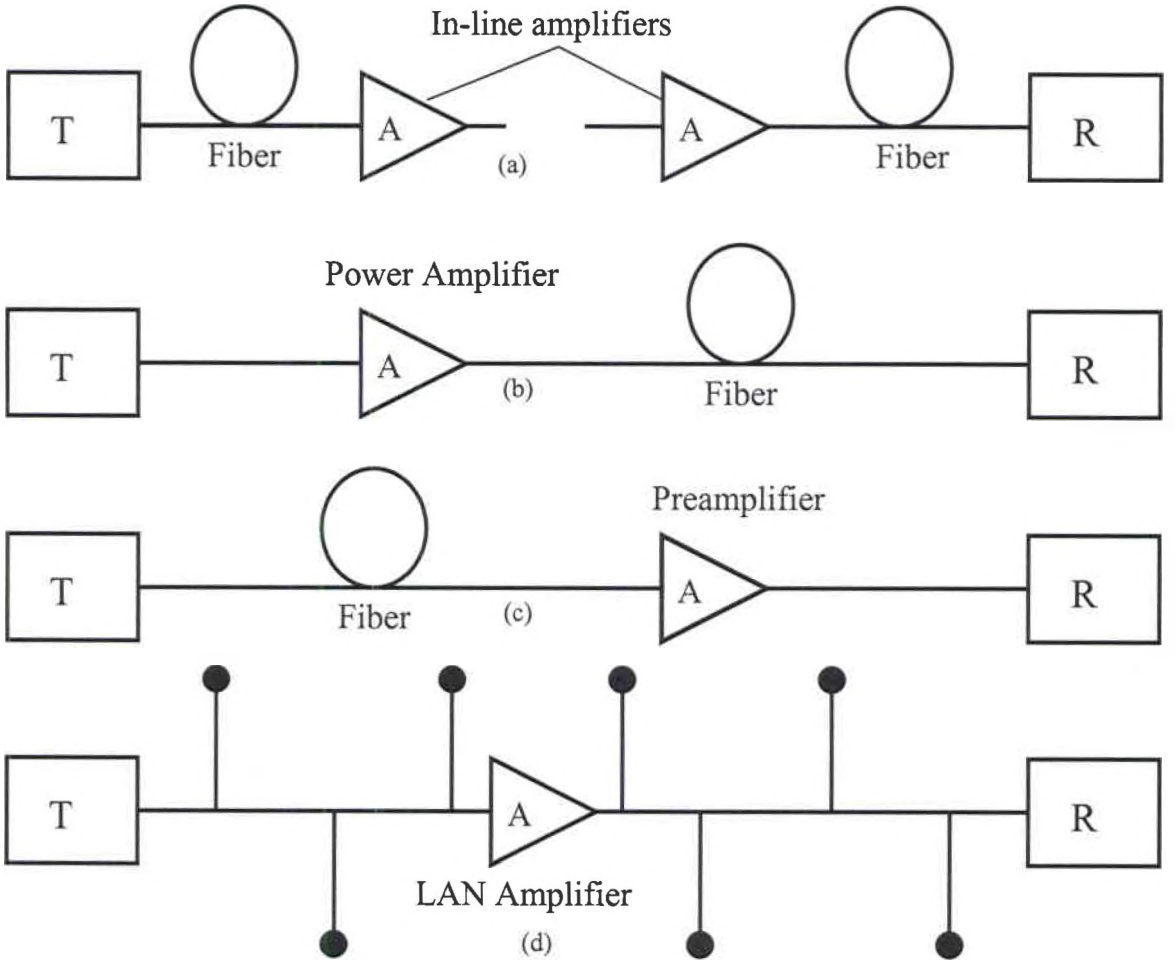

Fig. 2.1: Four possible applications of optical amplifiers in lightwave systems; (a) inline amplifiers,(b) booster amplifier,(c) preamplifier and (d) compensation of distribution losses in LAN [23].

2.1.3 Types of Optical Amplifiers

A number of different types of optical amplifiers have been studied [26]. These include:

- semiconductor laser amplifiers (SLA),
- fiber Raman amplifiers,
- fiber Brillouin amplifiers, and
- rare earth ion doped fiber amplifiers.

Semiconductor laser amplifiers:

SLAs provide high gain, large bandwidth, and lower current consumption with a high expected reliability and small size. SLAs are bidirectional amplifiers and can be used only as lumped amplifiers. Disadvantages of SLAs as compared to erbium amplifiers involve the interference between the adjacent pulses in the saturation regime due to the short gain recovery time. The short gain recovery time allows the amplification condition of a given pulse to affect only a relatively small number of the following time slots which results in a pulse pattern dependent intersymbol interference. This limits the maximum bit rate and reduces the acceptable input power. SLAs produce a significant pulse pattern distortion in the output signal at 25Gbps where no significant degradation was observed with erbium amplifiers over 100Gbps [30]. An additional disadvantage of SLAs is a large coupling loss between the SLA and the optical fiber. The losses degrade both the fiber to fiber gain and the effective noise figure. Losses can reach up to 10dB [31]. In view of the above, rare earth activated fibers find a major field of application as traveling wave fiber amplifiers for optical communications as an alternative to semiconductor laser amplifiers.

Raman amplifiers (RAs):

A fiber Raman amplifier uses stimulated Raman scattering (SRS) occurring in silica fibers when an intense pump beam propagates through it [32]. SRS differs from standard stimulated emission in one fundamental aspect: whereas in the case of standard stimulated emission, an incident photon stimulates the emission of another identical photon without losing its energy, in the case of SRS the incident pump photon loses its energy to create another photon of reduced energy at a lower frequency, the remaining

energy is absorbed by the medium in the form of molecular vibrations. Thus Raman amplifiers must be pumped optically to provide gain in contrast with SLAs which can be pumped electronically. An important difference from the case of SLA is that population inversion is not required for fiber Raman amplifiers. In fact, SRS is a nonresonant nonlinear phenomenon that does not require population transfer between energy levels. The Fig.2.2 shows schematically the operation of fiber Raman amplifiers and the energy level scheme.

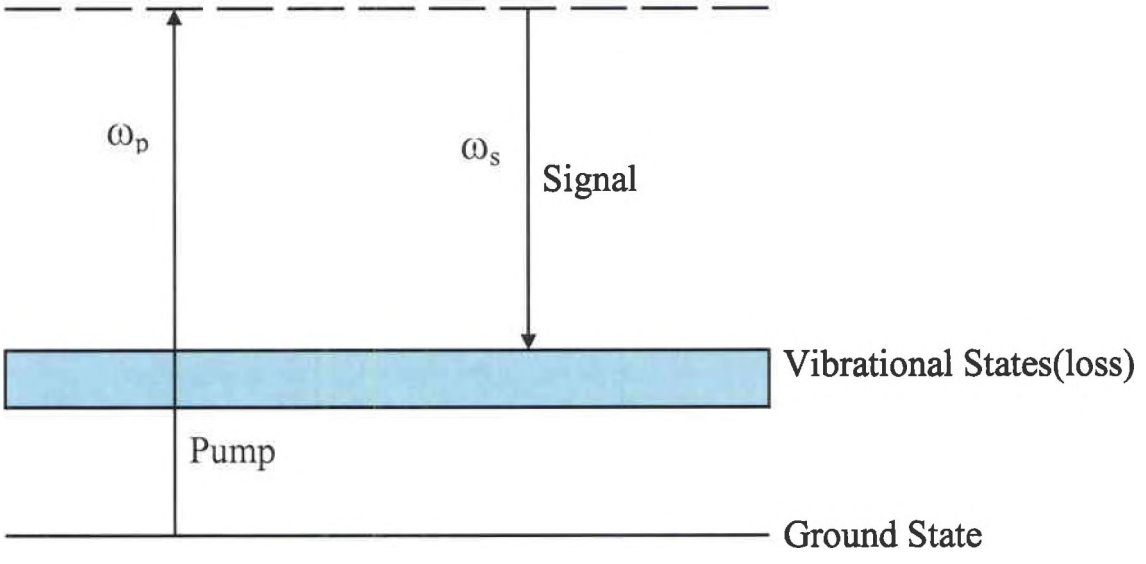

Fig. 2.2: The energy level scheme associated with SRS [23].

The pump and signal beam at frequencies ω_p and ω_s are injected into the fiber through a wavelength selective coupler. The energy is transferred from the pump beam to the signal beam through SRS as the two beams copropagate along the fiber. The pump and signal beams can also be injected in such a way that they counter propagate inside the fiber.

Both Raman amplifiers and erbium amplifiers amplify optical signals in the fiber by transferring energy from a pump to the signal. RAs have a low noise figure, low

connection loss, high gain, high output power, and broad bandwidth. The major drawback of RA's as compared to erbium amplifiers is their low efficiency (8dB fiber loss compensated with a 100mW pump power in an 80km fiber) [33].

Brillouin amplifiers (BAs):

Fiber Brillouin amplifiers are also pumped optically and a part of the pump power is transferred to the signal through SBS (stimulated Brillouin scattering). BAs are different from RAs in that the difference between the pump and signal frequencies is much smaller. The amplification process is similar and called stimulated Brillouin scattering. BAs provide high gain, high efficiency, and low connection loss. The major disadvantages are narrow bandwidths required for the pump signal, a large noise figure due to the thermal noise, and a low output power [34].

Both the Raman scattering and the Brillouin scattering are examples of inelastic scattering during which the frequency of the scattered light is shifted downward. Both of them can be understood as scattering of a photon to a lower energy photon such that the energy difference appears in the form of a phonon. The main difference between the two is that optical phonons participate in Raman scattering whereas acoustic phonons participate in Brillouin scattering. SBS also differs from SRS in the aspect that the amplification occurs only when the signal beam propagates in a direction opposite to that of the pump beam. Both scattering processes result in a loss of energy at the incident frequency and constitute a loss mechanism for optical fibers. However, the scattering cross sections are sufficiently small that power loss is negligible at low power levels. At higher power levels the nonlinear phenomena of stimulated Raman scattering and stimulated Brillouin scattering can lead to considerable fiber loss.

Erbium Doped Fiber Amplifiers (EDFAs):

A relatively new class fiber amplifiers make use of rare earth ions as a gain medium. These ions are doped inside the fiber core during the manufacturing process and pumped optically to provide the gain. The amplifier characteristics such as the operating wavelength and the bandwidth are determined by the dopants rather than by the silica fiber, which plays the role of the host medium. Many different rare earth ions, such as erbium, holomium, neodymium, samarium, thulium and ytterbium can be used to realize fiber amplifiers operating at different wavelengths covering visible to infrared region. Erbium doped fiber amplifiers [35] have attracted the most attention among them simply because they operate near 1.55μm, the wavelength region in which the fiber loss is minimum.

Erbium amplifiers demonstrate advantages over traveling wave semiconductor laser amplifiers (SLA), Raman amplifiers and Brillouin amplifiers. Overall Erbium amplifiers have better crosstalk characteristics, higher power operation, and a lower insertion loss than SLA's, higher efficiency than FA's and a broader bandwidth and lower noise figure than FAs. In addition, erbium amplifiers are the only amplifiers that can be used as both a distributed and lumped amplifier in telecommunications [31]. The summary of the properties of the amplifiers is tabulated as shown in the Table 2.1.

Table 2.1: Summary of the advantages and disadvantages of different types of amplifiers

Type of Amplifier	Advantages	Disadvantages
SLAs	High gain, large bandwidth, high reliability and small size	Pulse pattern distortion, large coupling loss, degraded NF and high losses.
Raman Amplifiers	Low NF, low connection loss, high gain, high output power and broad bandwidth.	Low efficiency
Brillouin Amplifiers	High gain, high efficiency and low connection loss.	Narrow bandwidth, large NF and low output power.
EDFAs	Minimum fiber loss, improved crosstalk characteristics, higher power operation, lower insertion loss, higher efficiency, broader bandwidth and lower NF.	

2.2 Architecture of EDFA

The basic EDFA architecture is illustrated in the Fig. 2.3.

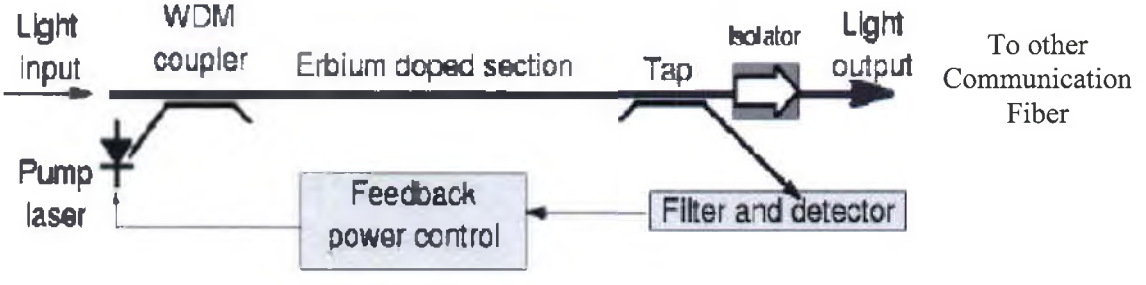

Fig. 2.3: Architecture of an EDFA implementation [48].

In the above schematic, a WDM coupler is always present, and provides a means of injecting the 980 nm pump wavelength into the length of erbium-doped fiber. It also

allows the optical input signal to be coupled into the erbium-doped fiber with minimal optical loss. The erbium-doped optical fiber is usually tens of meters long. The 980 nm energy pumps the erbium atom into a slowly decaying, excited state. When energy in the 1550 nm band travels through the fiber it causes stimulated emission of radiation, much like in a laser, allowing the 1550 nm signal to gain strength. The erbium fiber has relatively high optical loss, so its length is optimized to provide maximum power output in the desired 1550 nm band [24]. The tap that goes to detector is used to monitor the optical output power. The optical isolator is placed to monitor reflections back into the EDFA. This feature can be used to detect if the connector on the optical output has been disconnected. All these components have single mode fiber pigtails and are spliced together.

2.3 Characteristics of EDFA

The characteristics of an EDFA are essentially determined by the amplifier gain, saturation, and noise properties; all three are generally coupled together. Ideally, the EDFA should yield the highest gain possible, while having the highest saturation output power and lowest noise possible. The combined EDFA characteristics of gain, saturation power and noise are often referred as the EDFA performance. The spectroscopy of Er doped glass fibers plays a fundamental role in the analysis and physical understanding of optical fiber amplifiers. All the important device characteristics of EDFA may be evaluated via spectroscopic properties.

2.3.1 Spectroscopy of Erbium:

The energy levels corresponding to each possible atomic state for Er: glass are shown in the Fig. 2.4 [27]. The figure also shows possible absorption transitions in the visible and near infrared as well as possible radiative transitions. It shows the transition with center wavelength of 1.540nm, relevant to optical communications, originates from the $^4I_{13/2}$ level and terminates in the $^4I_{15/2}$ ground level. The pump absorption transition is justified near 1.480nm when considering the Stark level substructure of the $^4I_{13/2}$ and $^4I_{15/2}$ levels.

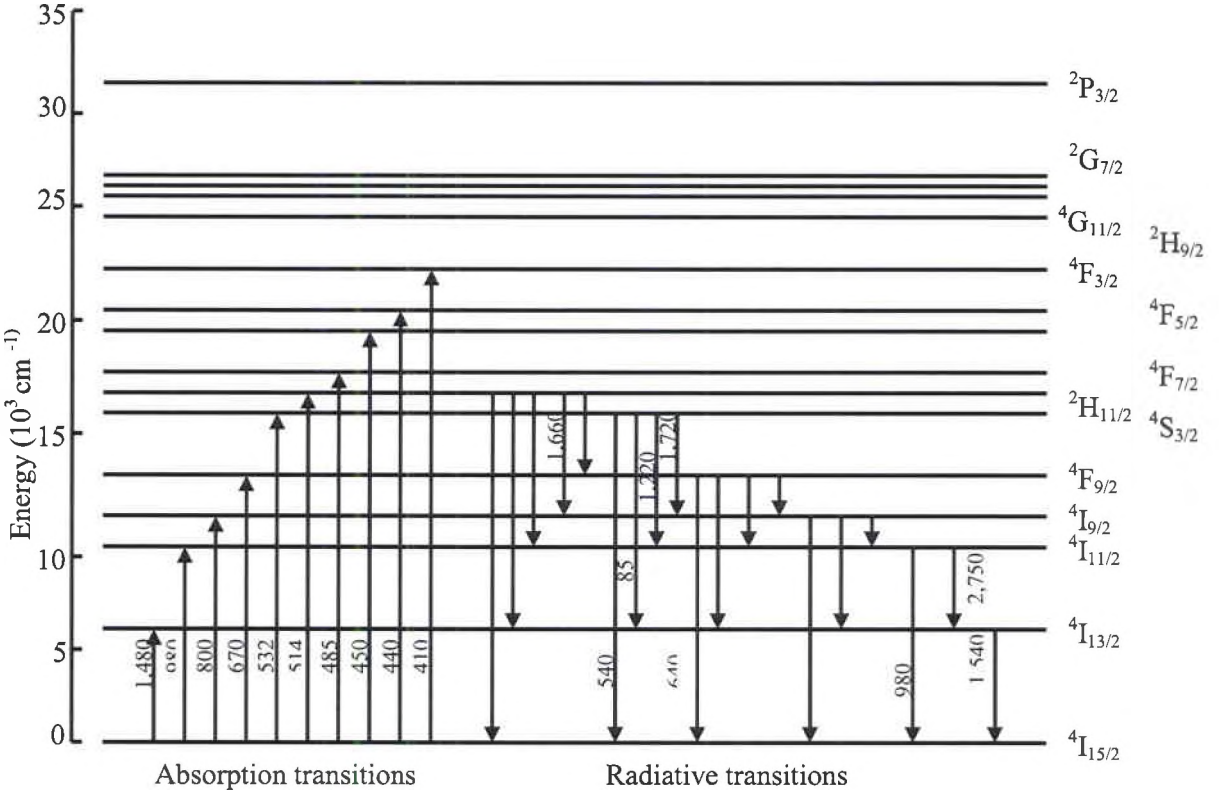

Fig. 2.4: Energy level diagram of Er:glass showing transitions [27].

Er^{3+} is the ion of choice for lasing and amplification in the 1.5μm region, due to its $^4I_{13/2} \leftrightarrow {}^4I_{15/2}$ transition. The various absorption bands seen in this spectrum correspond

to the absorption transitions shown in the Fig. 2.4. The broad and intense absorption band near 1.530μm indicates that Er^{3+}: glass is a strongly absorbing medium when not activated by any pumping mechanism.

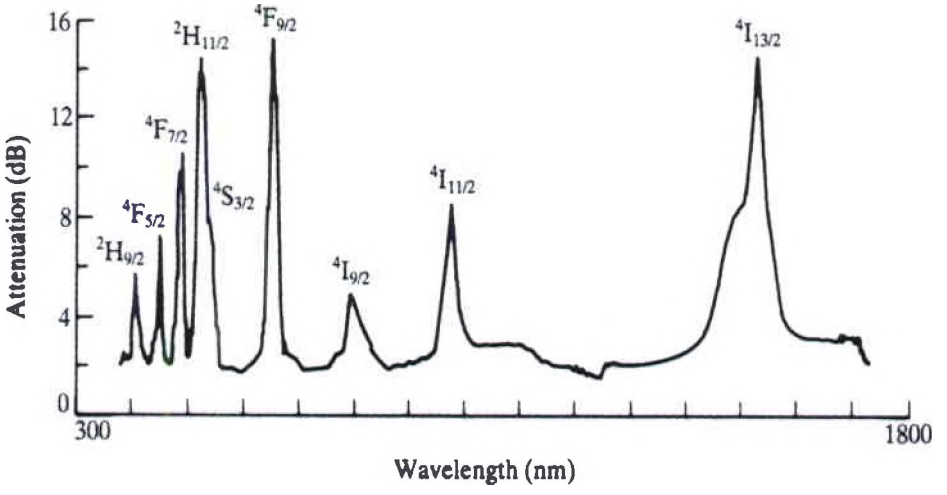

Fig. 2.5: Absorption spectrum of aluminosilicate Er^{3+}: doped fiber. The discrete absorption bands correspond to the transition shown in Fig. 2.4 [24].

The key to the success of erbium is that the upper level of the amplifying transition, $^4I_{13/2}$, is separated by a large energy gap from the next lowest level, making it a metastable state so that its lifetime is very long and mostly radiative. The value of the lifetime is around 10ms and varies depending on the host and the erbium concentration. This long lifetime permits the inversion of the population between the $^4I_{13/2}$ and $^4I_{15/2}$ with an *a priori* weak and thus practical, pump source.

2.3.2 Gain versus Pump Power:

The gain versus pump power is the first and most important measure of the EDFA performance [27]. Input pump power refers to the pump power at the input of the EDFA. Absorbed pump power is the difference

$$P_p^{abs} = P_p^{in} - P_p^{out}$$

(2.4)

For EDFAs, absorbed pump power is generally not relevant, since the amount of unabsorbed pump power due to bleaching can be significant in some cases. Thus, expressing the gain characteristics as a function of absorbed pump power does not reflect how much launched pump power is necessary to achieve the result. There exists an optimum wave length near λ = 665nm (see Fig. 2.5) for which the gain is maximized and this corresponds to the peak absorption wavelength. But at high pumps, near 980nm and 1480nm, the gain is nearly independent of the pump wavelength and this reflects a condition of full population inversion along the fiber. The Fig. 2.6 [37] shows the EDFA gain versus absorbed pump power for different EDFA lengths at the peak signal wavelength λ = 1531nm, corresponding to an Al-Ge-doped glass EDF.

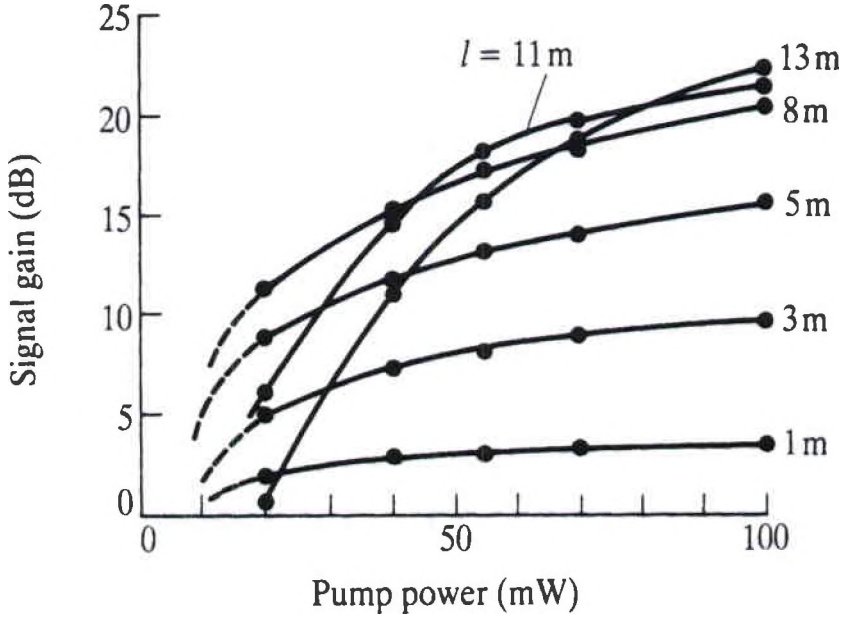

Fig. 2.6: Signal gain at λ = 1.531μm versus input pump power at λ = 514nm for different fiber lengths [24].

The most important feature of these measurements is the existence of an optimum length L_{opt}, different for each input pump power, for which the signal gain is maximized for amplifier lengths $L>L_{opt}$, the signal is reabsorbed along the fiber, as a result of an absence of population inversion in the fiber section, corresponding to a greater population in the $^4I_{15/2}$ ground level.

2.3.3 Gain versus Signal Power and Amplifier Saturation:

When EDFAs are operated in the small signal regime, the gain is independent of the input signal power [27]. The effect of increasing the input signal power P_s^{in} on the EDFA gain can be characterized by the expression

$$P_s^{out} = f(P_s^{in}) , \quad G = f(P_s^{in}) \text{ or } G = f(P_s^{out}) \tag{2.5}$$

In the small signal regime these expressions are linear.

$$P_s^{out}(P_s^{in}) = \text{const. x } P_s^{in} , \quad G(P_s^{in}) = G(P_s^{out}) = \text{const.} \tag{2.6}$$

Gain saturation is reached when the EDFA characteristics depart from those linear relations. The powers are expressed in decibel – mW or dBm units, according to the definition

$$P(\text{dBm}) = 10 \log_{10} [P(\text{mW})/P_0] , \text{ with } P_0 = 1\text{mW}. \tag{2.7}$$

Another parameter in EDFA, which is the saturation output power P_{sat}^{out}, is defined as the output power for which the EDFA gain has dropped by -3dB below its

unsaturated value G_{max}. The power P_{sat}^{out} is also referred to as saturated output power for 3dB gain compression. The parameter P_{sat}^{in} which is input saturation power is defined as for which the gain saturation or compression is -3dB. The two parameter set G_{max} and P_{sat}^{in} or P_{sat}^{out} which corresponds to a given or available LD pump power determine the EDFA power dynamic range. P_{sat}^{out} should not be confused with the EDFA saturated output power defined as the maximum output signal power that can be achieved under given experimental conditions. EDFAs that are operated in the saturation regime in order to yield a maximized output signal power are referred to as power amplifiers. For power EDFAs the power conversion efficiency is defined as the ratio

$$PCE = (P_s^{out} - P_s^{in}) / P_p^{in} \tag{2.8}$$

2.3.4 ASE Noise and Noise Figure:

The amplified spontaneous emission and the optical noise figure comprise the third most important characteristic feautures of EDFAs. The ASE power spectrum provides useful information on the EDFA operating characteristics in various pump and signal power regimes. The NF represents a measure of the SNR degradation from the input to the output of the amplifier. System applications require that a certain level of SNR be achieved at the receiver end. The ASE noise falling into the operating signal bandwidth represents a major parameter according to which the overall system performance can be determined.

Amplified spontaneous emission (ASE):

ASE arises from the fact that all the excited ions can spontaneously relax from the upper state to the ground state by emitting a photon that is uncorrelated with the signal photons. As shown in Fig 2. this spontaneously emitted photon can be amplified as it travels along the fiber and stimulates the emission of more photons from excited ions, viz., photons that belong to the same mode of the electromagnetic field as the original spontaneous photon. This parasitic process which can occur at any frequency within the fluorescence spectrum of the amplifier transitions reduces the gain from the amplifier. It robs photons that would otherwise participate in stimulated emission with the signal photons. This limits the total amount of gain available from the amplifier. Under normal condition the probability of spontaneous emission is higher than stimulated emission.

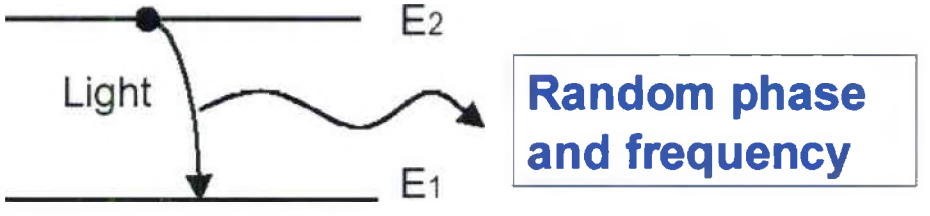

Fig2.7: Schematic representation of ASE [48].

2.4 Four Level Fiber Amplifier for 1.3μm

The rare earth ions that have been used for the optical amplifiers for 1.3μm signal wavelength all operate on the four level laser principle. The two principal candidates are Praseodymium (Pr^{3+}) and Neodymium (Nd^{3+}) all doped in a nonsilica host [24]. Pr^{3+} has received the most attention among the two ions. But these ions have low efficiency when compared to the EDFA and this necessitates higher pump levels for these amplifiers.

Another factor is the need for fluoride fiber processing and fabrication technology, which is less widespread and more complex than that of silica fibers.

2.4.1 Gain in a Four Level System:

The fundamental differences between the PDFA, NDFA and the EDFA arise because of the differences in the gain process between a four level amplifier and a three level amplifier.

Let us consider a four level system shown in the Fig 2.8 [24], with a ground state denoted by 0, an intermediate state into which energy is pumped, labeled 3, the upper level of the amplifying transition, labeled state 2, and the lower level of the amplifying transition, labeled state 1. The populations of these levels will be labeled N_i. The spontaneous transition rates between the various levels are denoted by τ_{32}, τ_{21}, τ_{10}, and τ_{20}. The total spontaneous transition rate out of level 2, τ_2, is obtained from the transition rates to levels 1 and 0, given by τ_{21}, τ_{10}.

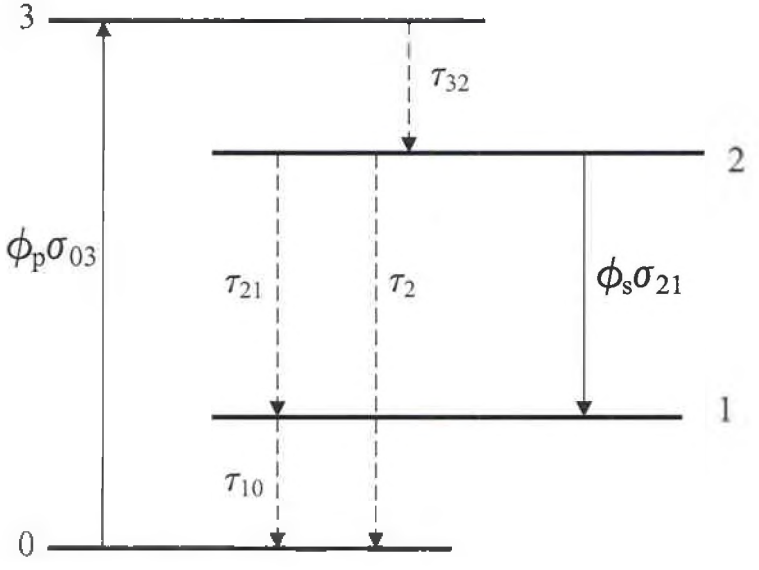

Fig 2.8: Four level system used for the amplifier model [24].

$$1/\tau_{32} = 1/\tau_{21} + 1/\tau_{20}$$

(2.9)

We assume a fast relaxation rate from level 3 to level 2, so that $N_3 \sim 0$. We also assume that level 1 empties into level 0 at a fast rate so that we can write in addition that $N_1 \sim 0$. We then have $N_0 + N_2 = N$ where N is the total population. For small signal gains, the population inversion is given by

$$N_2 \sim N_2 - N_1 \sim (\tau_2 \sigma_{03} \phi_p)/ (1+ \tau_2 \sigma_{03} \phi_p)$$

(2.10)

In contrast to a three level system, the population inversion in a four level system is always positive, as shown in the Fig.2.9.

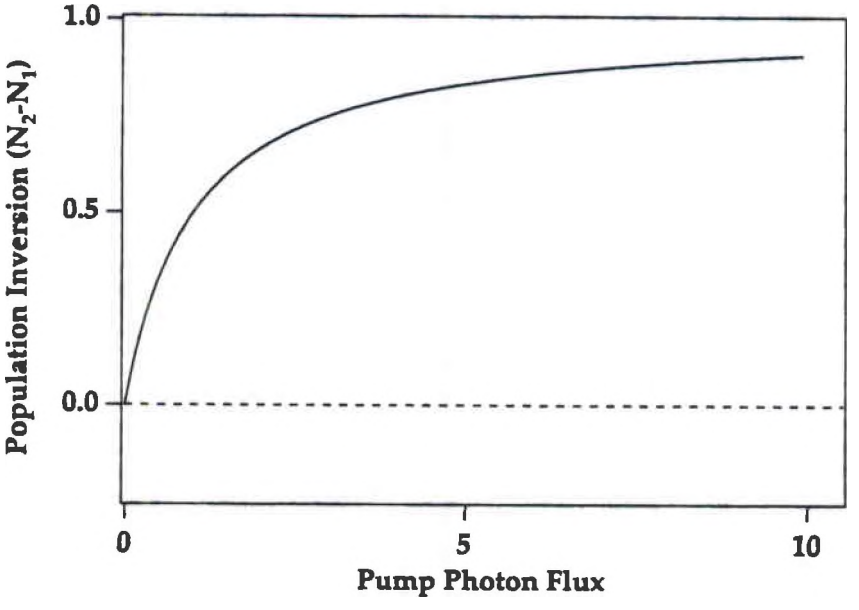

Fig 2.9:Population inversion in an ideal system [24].

In the case where the pump power is zero, the signal should suffer no attenuation and no gain. Thus, an advantage of a four level fiber amplifier as is true with Pr^{3+} or Nd^{3+}

ions over an erbium doped fiber amplifier is that in the event of a pump source failure the former becomes transparent whereas the latter becomes a strong absorber. As soon as the pump power becomes infinite, the signal experiences gain. In practice, the situation is complicated by the fact that there is usually some nonzero background loss, such that even with zero pump power the signal experiences some absorption in a four level amplifier ion doped fiber. Thus a small amount of pump power is needed to render the active medium transparent in an EDFA. The small signal gain after the signal has traversed a section of pumped amplifier fiber is

$$g = (\sigma_{em}\, \tau\, P_{abs}\, F)/ (h\upsilon_p A_{eff}\, \eta_p) \tag{2.11}$$

where σ_{em} is the emission cross section, τ is the upper state lifetime, $h\upsilon_p$ is the pump photon energy, A is the fiber core area, P_{abs} is the absorbed pump power in the section of fiber considered, F is the overlap integral between the pump and signal fields in the traverse dimensions, and η_p is the fractional pump energy that propagates in the fiber core [38]. Finally, it must be noted that for most four level fiber amplifiers, an ideal four level system does not take into account the following complex effects

- a finite population in level 1,
- signal excited state absorptions,
- pump excited state absorption,
- competing fluorescent transitions between other levels.

2.4.2 Pr^{3+} Doped Fiber Amplifiers:

The energy level diagram of Pr^{3+} is shown in Fig.2.10

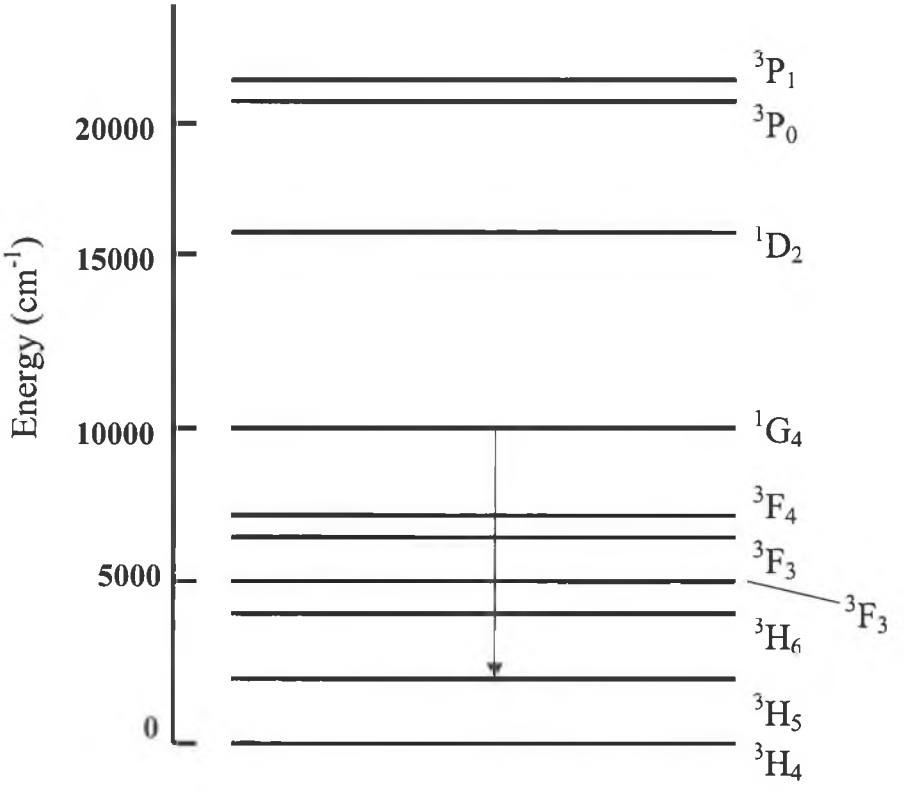

Fig.2.10: Energy level diagram of Praseodymium showing the 1.3 μm transition[24].

The transition between levels $^1G_4$ and $^3H_5$ is very short and there is no prospect of obtaining sufficient population inversion on the $^1G_4$ – $^3H_5$ transition. This is due to nonradiative relaxation from the $^1G_4$ level to the levels directly below it, i.e. the $^3F_{4,3,2}$ levels. This can be contrasted with the case of Er^{3+}, where there are no intermediate levels lying between the two levels of the amplifying transition, eliminating the possibility for a multitude of nonradiative decay processes.

The Pr^{3+} doped fiber amplifier was first demonstrated by Ohishi and coworkers and by other groups [39]. Gains in excess of 30dB have been observed for pump powers on the order of several hundreds of mW. Laser diode pumping has been demonstrated. A gain of 28dB was obtained when pumping with four 1.02μm laser diodes, and a one laser

diode pumped double pass configuration module was shown to have a gain of 23dB [40]. A gain of 40dB was obtained with a two stage Pr^{3+} fiber amplifier with each stage pumped by a solid state Nd: YLF laser. In a latter demonstration by the same group a saturated signal output power of 20dB was obtained as well as a small signal noise figure of 5dB, at 1.30μm [41]. High gain and high output power Pr^{3+} fiber amplifiers using high power MOPA laser diodes as pumps have also been demonstrated [42].

2.4.3 Nd^{3+} Doped Fiber Amplifiers:

Nd^{3+} doped fiber amplifiers were early candidates as amplifiers at 1.3μm. But unfortunately they suffer from a host of problems and have never yielded suitable gains at the wavelength of interest for transmission applications despite the fact that they can be pumped in the 800nm region where high power laser diodes are available. But the study of the Nd^{3+} based amplifiers has provided useful insights into the properties of rare earth doped fiber amplifiers. In addition to a very strong excited state signal absorption effect, Nd^{3+} suffers from the fact that another transition at a wavelength of 1.06μm, originates from the same $^4F_{3/2}$ upper state as the 1.3μm transition. The 1.06μm transition has, in fact an emission cross section about four times stronger than that at 1.3μm, and thus the 1.06μm transition tends to steal the gain from the 1.3μm transition. Even without these deleterious effects, the product of the emission cross section and the lifetime for Nd^{3+} is an order of magnitude lower than that for Er^{3+}, indicating that the pump efficiencies for an Nd^{3+} fluoride fiber amplifier will be significantly lower than what we are accustomed to for Er^{3+} doped fiber amplifiers at 1.5μm[43]. The Fig.2.11 shows the Nd^{3+} energy levels, along with the processes relevant to gain in an Nd^{3+} doped amplifier.

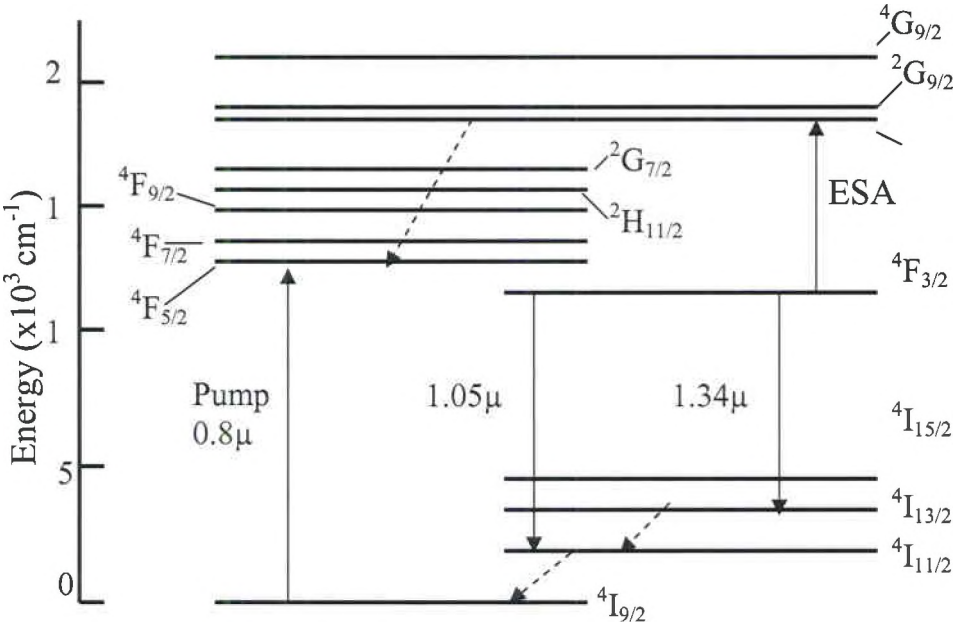

Fig. 2.11: Energy level diagram of neodymium and the relevant transition for 1.3μm for the amplification process [24].

A silica host for Nd^{3+} is not suitable because the excited state absorption in the 1.3μm region is very strong in silica. A Nd^{3+} doped fiber laser at 1.3μm was demonstrated in a fluoride host [44]. A gain of 4-5 dB was obtained with 150mW of pump at 795nm, for signal wavelengths between 1320 and 1350nm [45]. A gain of 3.3dB was also obtained at 1.32μm for only 50mW of pump power at 820nm [46]. The gain was then flat for pump powers above 50mW due to the increase in the 1.05μm ASE as shown in the Fig.2.12.

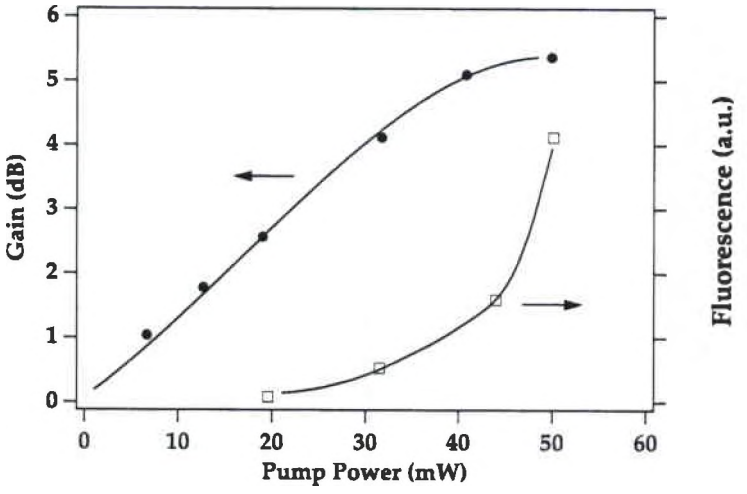

Fig.2.12: Gain at 1.3μm and fluorescence as a function of pump power in an Nd^{3+} doped fluoride fiber amplifier [24].

Amplifier investigations were carried out in an Nd^{3+} doped fluorophosphate host [47]. Only 3.4dB of gain is obtained at 1.32μm and the gain saturates for pump powers above 80mW due to the ASE buildup at 1050nm. Since the ASE at 1050nm is a major contributor to the low gain at 1.3μm in Nd^{3+} doped fiber amplifiers, attempts have been made to reduce it by introducing coupling notch filters; a gain enhancement of up to 5dB was achieved at a signal wavelength of 1328nm.

CHAPTER 3

SPATIAL EVOLUTION OF POWER IN EDFA

ANALYTICAL APPROACH

3.1 Introduction

The simplest treatment of the erbium doped fiber amplifier starts out by considering a three level atomic system [28]. Most of the important characteristics of the amplifier can be obtained from this simple model and its underlying assumptions. An added complication will be stimulated emission at the pump wavelength.

As mentioned, the erbium doped amplifier is modeled as a three level laser system. This model allows us to characterize the amplifier in terms of pump, signal and amplified spontaneous emission (ASE) powers [24]. The rate equations describing the effects of pump, signal and ASE powers on the population density in an erbium doped fiber amplifier is suggested.

In this chapter, these rate equations are solved by finding an appropriate solution with has no loss terms. The quasi analytical solutions of the rate equations are used to find power equations for pump, signal and ASE powers. Later, the evolution of powers with respect to distance is analyzed.

3.2 Modeling of EDFA as Three Level System

A three level system [24] is shown in Fig.3.1, with the ground state denoted by 1, an intermediate state labeled 3 (into which energy is pumped) and upper laser state 2.

Since state 2 often has a long lifetime in the case of a good laser or amplifier, it is sometimes referred to as a metastable level. Thus, state 2 is the upper level of the amplifying transition and state 1 is the lower level. The populations of the levels are labeled N_1, N_2 and N_3. This three level system is intended to represent that part of the energy level structure of Er^{3+} as was shown in chapter 2, Fig 2.4, that is relevant to the amplification process.

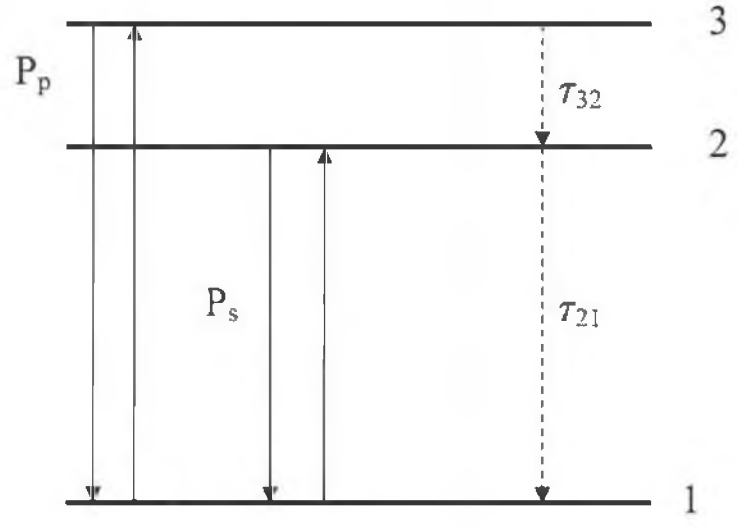

Fig 3.1: Three Level Laser Energy Level Diagram [24].

3.3 Quasi Analytical Solution of Power Equations

In this section we present quasi analytical solution derived by Franco et.al [26] for signal and ASE spectral power densities versus the propagating distance. The application of these solutions requires only a preliminary measurement of pump power, power absorption in the absence of signal. We also monitor the pump power at the EDFA output. The pump, signal, and ASE spectral density powers along the fiber in a three level laser satisfy [26]

$$\frac{dP_p(z)}{dz} = -\sigma_p N_1 \Gamma_p P_p(z),$$

(3.1)

$$\frac{dP_s(z)}{dz} = [\sigma_e N_2 - \sigma_a N_1]\Gamma_s P_s,$$

(3.2)

$$\frac{dP_a(z)}{dz} = [\sigma_e N_2 - \sigma_a N_1] \times \Gamma_s P_a + 2h\upsilon\sigma_e N_2 \Gamma_s,$$

(3.3)

where $N_{1,2}$ are the lower and upper laser level populations, $\sigma_{e,a}$ are the emission and absorption cross sections, σ_p is the absorption cross section at the pump wavelength, and $\Gamma_{s,p}$ is the overlap factor between signal and pump modes and the doped fiber core respectively.

The ASE and signal power depends on the power evolution of pump power. From (3.1) the pump power is straight forwardly obtained as:

$$P_p(z) = P_p(0)\exp(-\alpha z), \text{ where } \alpha = \sigma_p N_1 \Gamma_p$$

(3.4)

The parameter α may be determined experimentally by measuring the pump power at the EDFA output. Without input signal

$$\alpha = \frac{-1}{L}\ln\left[\frac{P_p(L)}{P_p(0)}\right]$$

(3.5)

Using α as in eq. (3.4) in eqs (3.2 and 3.3) leads to:

$$P_a(z) = \frac{2h\upsilon(K-\alpha C)}{(K-\alpha B)}\{\exp[(K-\alpha B)z]-1\},$$

(3.6)

$$P_s(z) = P_s(0)\exp[(K-\alpha B)z], \tag{3.7}$$

Where

$$K = \Gamma_s \sigma_e N_t,\ B = \Gamma_s \frac{\sigma_e + \sigma_a}{\sigma_p A_p},\ C = \Gamma_s \frac{\sigma_e}{\sigma_p \Gamma_p}$$

3.4 Signal and ASE Power Evolution

To understand the nature of solutions for power obtained in the previous section, we chose a set of practical parameters and plotted the evolution of signal and ASE graphically. Fig 3.2 and Fig 3.3 show the behavior of the ASE power and signal power densities obtained by the numerical solutions of the eqs. (3.1), (3.2) and (3.3) using the parameters listed in the Table 3.1.

Table 3.1 Values of the Parameters used to Generate Franco Plots

$\lambda_P = 514.5nm$	$\lambda_s = 1530nm$
$\sigma_p = 2.4\times10^{-21}cm^2$	$\sigma_a = 4.83\times10^{-21}cm^2$
$\sigma_e = 8.1\times10^{-21}cm^2$	$P_s = 100\mu W$
$\Gamma_s = \Gamma_p = 0.4$	$P_p = 50mW$
$N_1 = 9.02\times10^{20}m^{-3}$	$N_2 = 7.31\times10^{20}m^{-3}$

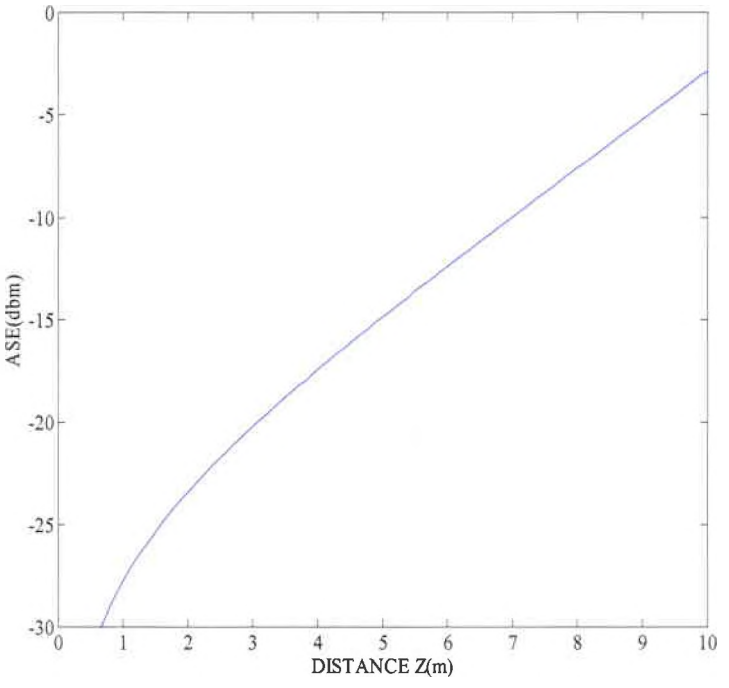

Fig 3.2 ASE evolution along the fiber length using Franco's Equations

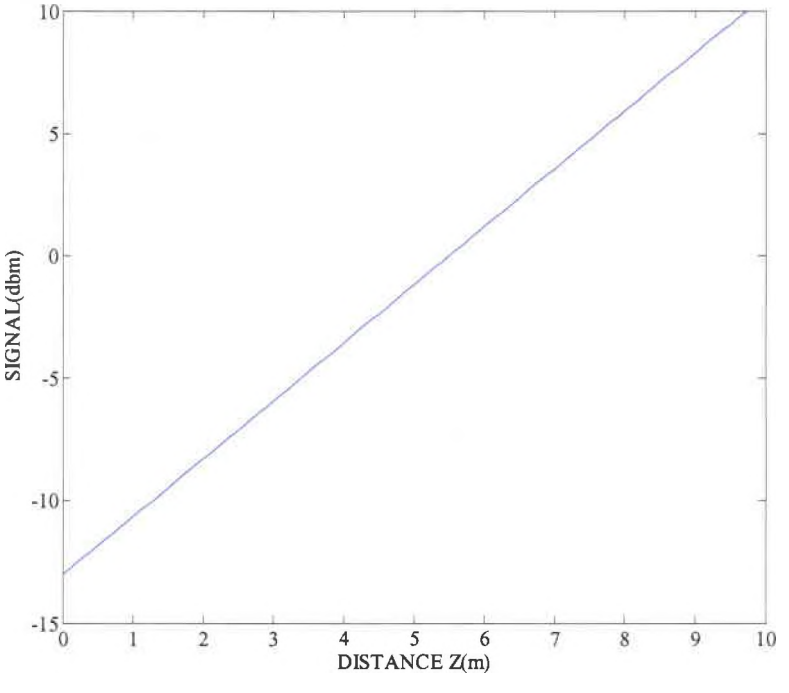

Fig 3.3 Signal Power evolution along the fiber amplifier length using Franco's Equations

CHAPTER 4

TEMPORAL AND SPATIAL EVOLUTION OF POPULATION AND POWER IN EDFA - A NUMERICAL APPROACH

4.1 Introduction

In chapter 3 we have analyzed rate equations for EDFAs by quasi analytical approach. In this chapter we use the EDFA model to obtain the population density and power evolution equations. These equations are then numerically solved assuming temporal steady state using MATLAB. The spatial evolution of the pump, signal and ASE powers, and thereafter the population density evolution of the ground (lower) and metastable (upper) levels for various initial conditions are analyzed and interpreted.

4.2 Rate Equations

The rate equations describing the effects of pump, signal and ASE powers on population density are given as follows [20]:

$$\frac{dN_1}{dt} = -\left[\frac{\sigma_{sa}\Gamma_s}{h\upsilon_s A}(P_s + P_a) + \frac{\sigma_{pa}\Gamma_p}{h\upsilon_p A}(P_p)\right]N_1 + \frac{\sigma_{pe}\Gamma_p}{h\upsilon_p A}(P_p)N_3 + \left[\frac{\sigma_{se}\Gamma_s}{h\upsilon_s A}(P_s + P_a) + A_{21}\right]N_2 + \frac{\sigma_{pe2}\Gamma_p}{h\upsilon_s A}(P_p)N_2 \tag{4.1}$$

$$\frac{dN_2}{dt} = \frac{\sigma_{sa}\Gamma_s}{h\upsilon_s A}(P_s + P_a)N_1 - \left[\frac{\sigma_{se}\Gamma_s}{h\upsilon_s A}(P_s + P_a) + A_{21}\right]N_2 - \frac{\sigma_{pe2}\Gamma_p}{h\upsilon_p A}(P_p)N_2 + A_{32}N_3 \quad (4.2)$$

In the above equations, the absorption and emission cross sections of the signal and pump are $\sigma_{s,\,p;\,a,\,e,\,e2}$. With pumping into the metastable level, the amplifier behaves as a two level system and

$\sigma_{pe2} = \sigma_{pe}$. Pumping into other absorption bands have $\sigma_{pe2} = 0$. Other parameters are the fiber core area A, the signal to core overlap Γ_s, and the pump to core overlap Γ_p. The parameters Γ_s and Γ_p are small since the erbium ions are considered to be confined to the region of the optical mode's peak intensity. The nonradiative transition rate from level 3 to 2 is A_{32} and the radiative transition rate from level 2 to 1 is A_{21}.

4.3. Pump Configurations

Three different pump configurations are possible for pumping a length of erbium doped fiber. These are: copropagating pump and signal, counter propagating pump and signal, and bi-directional pumping, as depicted in the Fig. 4.1 (a), (b) and (c). As far as small signal gain is concerned, copropagating and counterpropagating pumps yield the same gain and only the total amount of pump power matters. This is because the ASE patterns generated by the two pump patterns are mirror images of each other and so the average upper state population is the same in both the cases. When the fiber is sufficiently long, bi-directional pumping results in higher small signal gain at 1.5μm for equal amounts of pump power than either the co or counter propagating pumping patterns.

The copropagating pump configuration offers the lowest noise figure because the portion of the fiber that the signal enters tends to be more inverted than the section by which the signal exits. Thus the signal undergoes more gain per unit length at the beginning of the fiber than at the exit. In the counter propagating configuration, lower gain per unit length at the beginning of the fiber is equivalent to having some amount of loss for the signal before it enters the amplifier. Any loss that the signal experiences at the beginning of the fiber will degrade the noise figure. Thus, in the absence of any other effects, the copropagating pump configuration is preferred for obtaining a low noise figure.

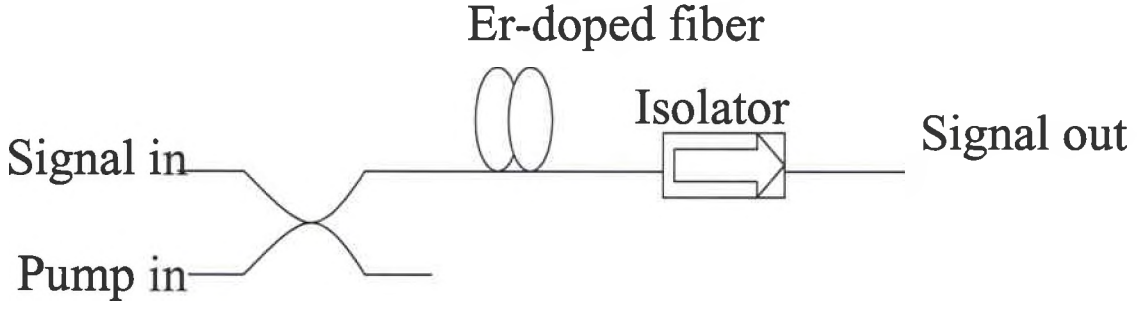

Fig 4.1 (a): Copropagating Pump and Signal [24].

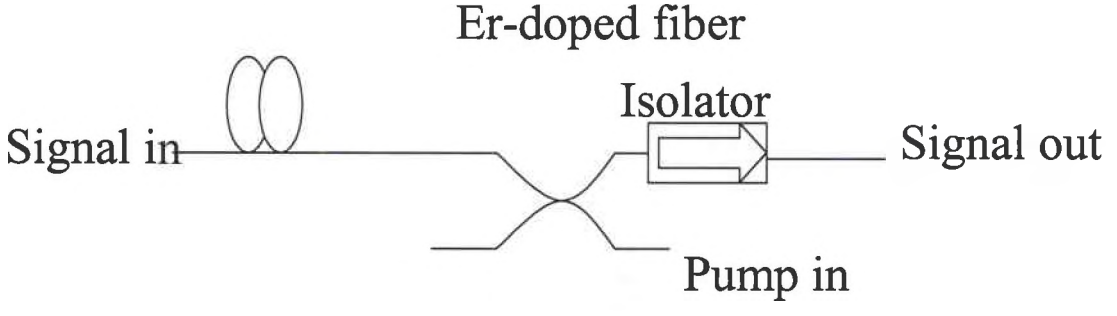

Fig 4.1 (b): Counter Propagating Pump and Signal [24].

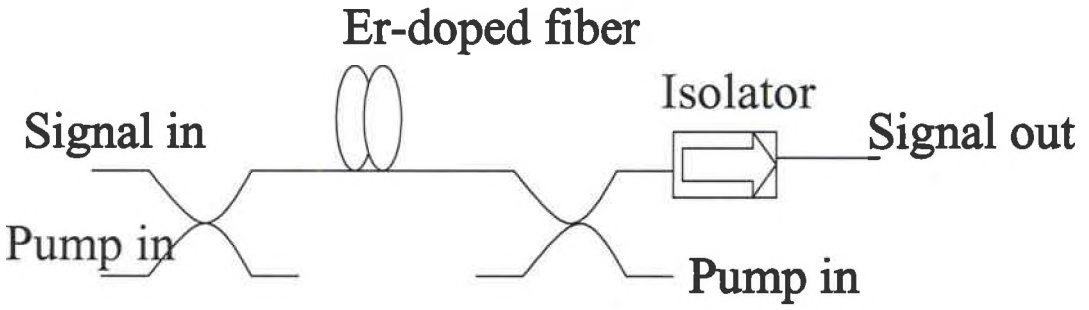

Fig 4.1 (c): Bidirectional Pump [24].

4.4 Solution for the EDFA Rate Equations - Numerical Representation

In steady state, we assume N_1 and N_2 to be independent of time. This can be justified since the settling period of the population densities is in the order of $10^{-5} - 10^{-6}$ sec [49]. Thus,

$$\frac{dN_1}{dt} = 0, \text{ and} \tag{4.3}$$

$$\frac{dN_2}{dt} = 0. \tag{4.4}$$

Consider also

$$N_3 = N_t - N_1 - N_2, \tag{4.5}$$

Where N_t is the total population of particles (erbium ions). By grouping the coefficients for the population densities individually yields eq. (4.6) and eq. (4.7) from eqs. (4.1 and 4.2) respectively.

$$0 = -N_1\left[\frac{\sigma_{sa}\Gamma_s}{h\upsilon_s A}(P_s+P_a)+\frac{\sigma_{pa}\Gamma_p}{h\upsilon_p A}(P_p)+\frac{\sigma_{pe}\Gamma_p}{h\upsilon_p A}(P_p)\right] + N_t\left[\frac{\sigma_{pe}\Gamma_p}{h\upsilon_p A}(P_p)\right] + N_2\left[\frac{\sigma_{se}\Gamma_s}{h\upsilon_s A}(P_s+P_a)+A_{21}\frac{\sigma_{pe}\Gamma_p}{h\upsilon_s A}(P_p)-\frac{\sigma_{pe}\Gamma_p}{h\upsilon_p A}(P_p)\right],$$

(4.6)

$$0 = N_1\left[\frac{\sigma_{sa}\Gamma_s}{h\upsilon_s A}(P_s+P_a)-A_{32}\right] - N_2\left[\frac{\sigma_{se}\Gamma_s}{h\upsilon_s A}(P_s+P_a)+A_{21}+\frac{\sigma_{pe2}\Gamma_p}{h\upsilon_p A}(P_p)+A_{32}\right] + A_{32}(N_t).$$

(4.7)

The propagation equations [20] for the pump, signal and ASE field powers are given as:

$$\frac{dP_p}{dz} = -P_p\Gamma_p(\sigma_{pa}N_1-\sigma_{pe2}N_2-\sigma_{pe}N_3) - \alpha_p P_p,$$

(4.8)

$$\frac{dP_s}{dz} = P_s\Gamma_s(\sigma_{se}N_2-\sigma_{sa}N_1) - \alpha_s P_s \text{ , and}$$

(4.9)

$$\frac{dP_a}{dz} = P_a\Gamma_s(\sigma_{se}N_2-\sigma_{sa}N_1) + 2\sigma_{se}N_2\Gamma_s h\upsilon_s\Delta\upsilon - \alpha_s P_a.$$

(4.10)

The α_s and α_p represent the internal loss terms. The second term in eq. (4.10) gives the ASE power produced in an amplifier per unit length. The power produced is within

the amplifier bandwidth $\Delta\upsilon$, which is homogeneously broadened. The internal loss of the amplifier usually corresponds to signal and pump attenuation in the transmission fiber. The values of all the parameters used in the eqs. (4.6 – 4.10) are given in Table 4.1 [20].

Table 4.1 Fiber Amplifier Parameters used in Calculations

$\lambda_P = 1480 \ \ nm$	$\lambda_s = 1545 \ \ nm$
$\sigma_{pe} = 0.42 \times 10^{-21} cm^2$	$\sigma_{pa} = 1.86 \times 10^{-21} cm^2$
$\sigma_{se} = 5.03 \times 10^{-21} cm^2$	$\sigma_{sa} = 2.85 \times 10^{-21} cm^2$
$A_{21} = 100 s^{-1}$	$A_{32} = 10^9 s^{-1}$
$A = 12.6 \times 10^{-8} cm^2$	$\Delta\upsilon = 3100 \ \ GHz(25 \ \ nm)$
$\Gamma_s = \Gamma_p = 0.4$	

The signal chosen for amplification is of the wavelength 1550 nm approximately, and a 1480 nm pump is used instead of 980 nm. This is because the 1480 nm pump provides a higher gain than the 980 nm pump [24]. The 1480 nm pump can maintain the necessary inversion levels over significantly longer lengths than the 980 nm pump. The reason for this is the higher quantum efficiency of 1480 nm pumping. This allows the signal to grow to a higher maximum value.

4.4.1 Numerical Approach

For the numerical approach, the rate of change of population levels with respect to time is neglected, thereby assuming steady state. However, the population levels are assumed to be varying with distance z. From eqs. (4.1 and (4.2), N_1 and N_2 are solved in terms of the pump, signal and ASE powers. Next, N_1 and N_2 are eliminated from eqs. (4.8

- 4.10) by replacing them with the expressions obtained from the previous step. These mutually coupled differential equations are then numerically solved for P_p, P_s and P_a as functions of distance z. The power values obtained versus z are then placed back into eqs. (4.6 and 4.7) to generate the population densities at the corresponding z values. To solve the coupled differential equations for power we have used symbolic math tool box MATLAB and then generated additional plots by varying different parameters. These results are discussed next.

4.5 Graphical Results and Analysis

Fig 4.2 (a) and (b) illustrates the pump (blue line), signal (red line) and ASE power (black line) of 50m long distributed amplifier when the initial ASE is assumed as 10^{-12}Watts and 10^{-15}Watts respectively. The pump and signal loss coefficients are taken to be 5.76 x 10^{-5} /m, and the initial pump power is 30mW.

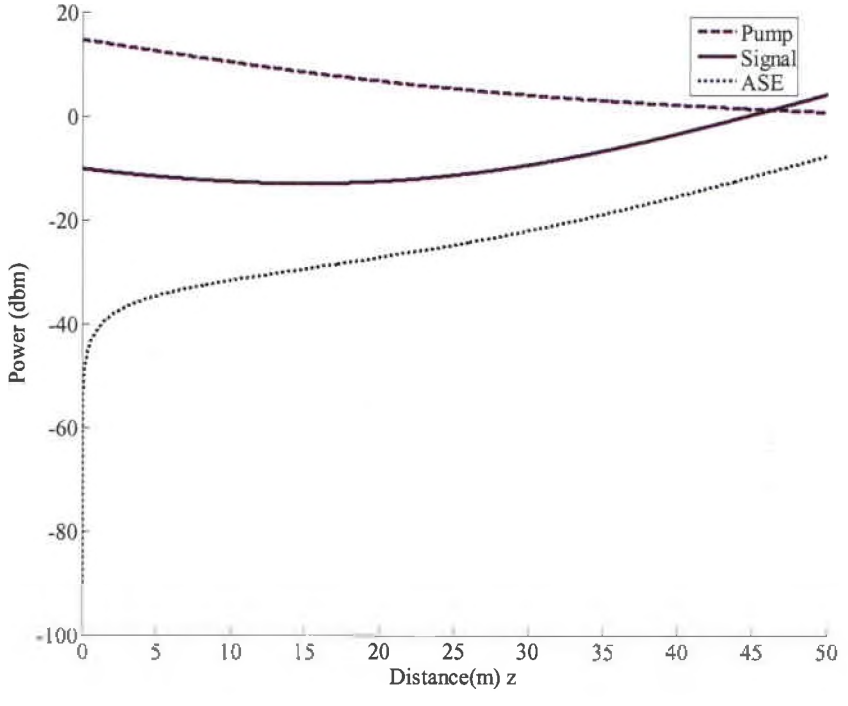

Fig 4.2(a): Evolution of Signal, Pump and ASE power for initial ASE as 10^{-12} Watts .

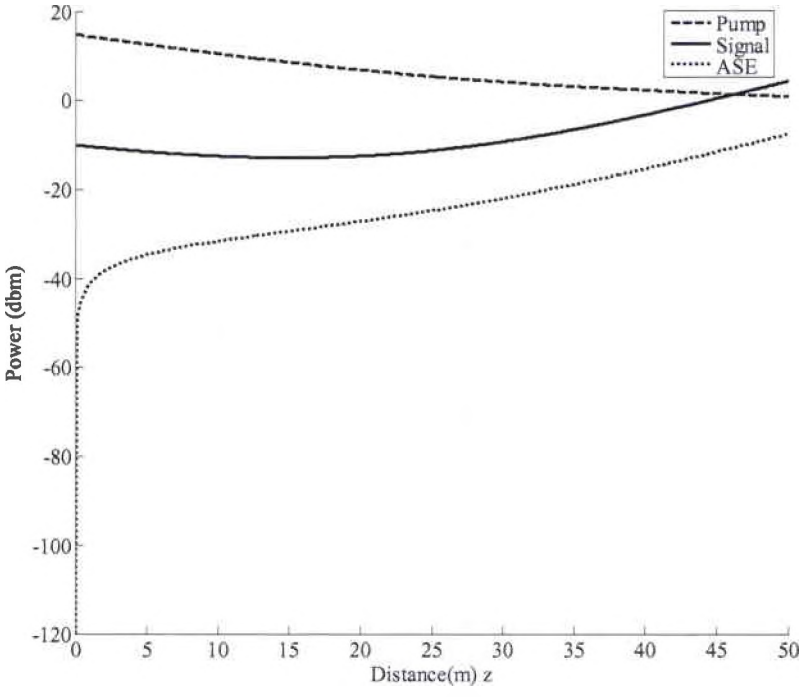

Fig 4.2(b): Evolution of Signal, Pump and ASE power for initial ASE as 10^{-15} Watts.

In order to achieve sufficient gain, the fiber is doped with $N_t = 2 \times 10^{18}/cm^3$. The input signal power is 100μw. From Fig 4.2 we can note that as distance increases there is a power transfer from pump to signal. A comparison between signal power and the ASE power shows that both increase at the same rate. This is expected since the ASE feeds the signal power.

4.5.1 Population Inversion

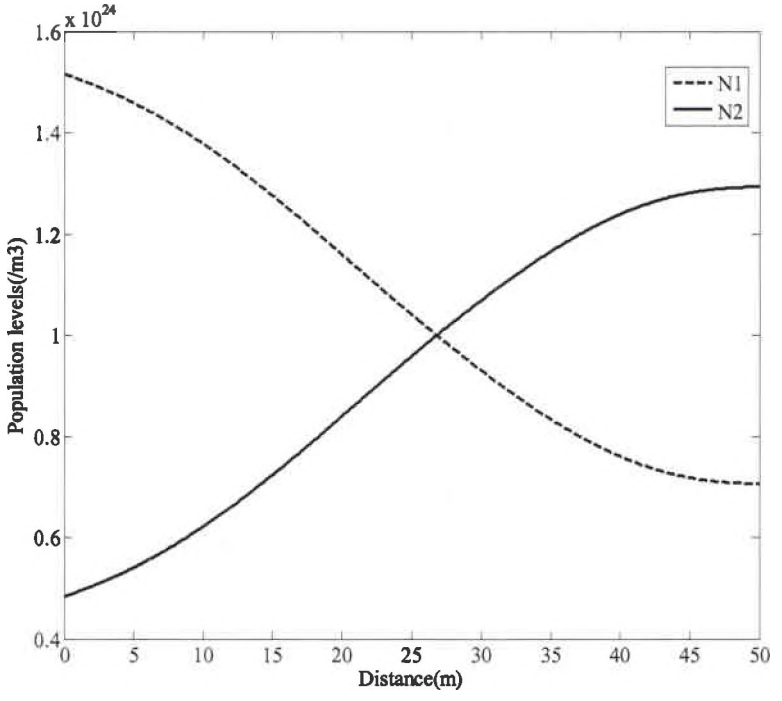

Fig 4.3: Population Evolution of Ground level (N_1) and Metastable level (N_2) in EDFA

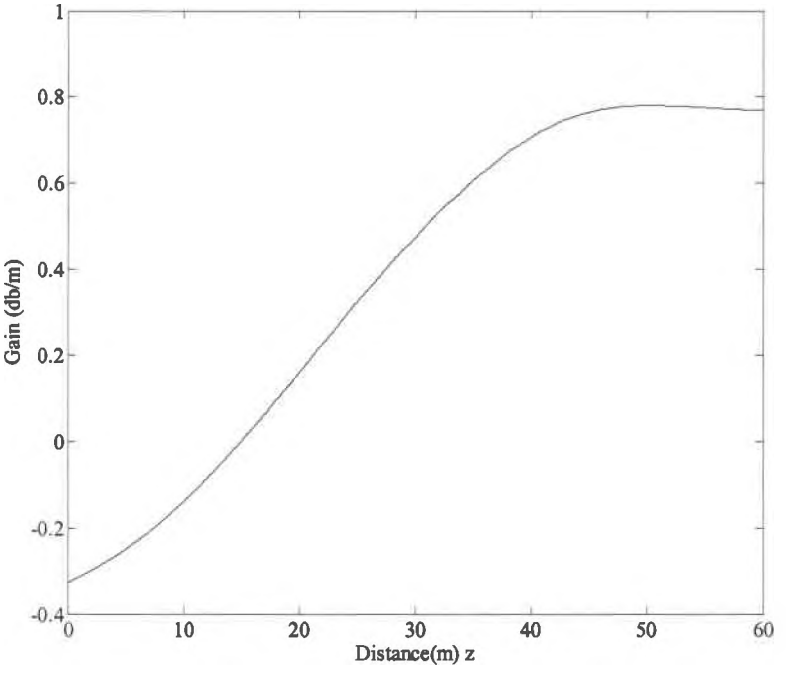

Fig 4.3 (a): Gain Plot for EDFA

Fig 4.3 illustrates the change in population densities in the ground level (N_1) and metastable level (N_2) as a function of distance. By observing the above figure the population inversion occurs around 27m from the starting of the fiber. N_2 increases along the fiber length and saturates at a maximum level ($1.28\text{x}10^{24}/\text{m}^3$). N_1 decreases with the fiber length and reaches a minimum level ($7.2\text{x}10^{23}/\text{m}^3$). This plot verifies that the sum of the population densities in the metastable and ground levels is equal to the doped total population density, i.e., at any point along the fiber the sum of N_1 and N_2 is always approximately equal to $N_t = 2\text{x}10^{24}/\text{m}^3$ (we neglect N_3, assuming a fast state). In Fig 4.3 (a) the gain increases and reaches to a saturation value. As the population densities saturate the gain also saturates which is called the constant amplification region. We can notice from the Fig 4.3 and Fig 4.3 (a) that the saturation in both the population densities and the gain occur at the same distance. Fig 4.4 depicts a series of population inversion plots with different values of total population density. From the plots in Fig 4.4, we conclude that as the doping increases the population inversion occurs earlier. The above observation is to some extent compatible with expected behavior, since gain is proportional to population inversion. At higher dopant density, gain is achieved rapidly along z. As the population density is decreased population inversion is occurring at a farther distance indicating that the gain is being delayed. The population densities used in the Fig 4.4 are $9\text{x}10^{16}/\text{cm}^3$, $7.5\text{x}10^{17}/\text{cm}^3$, $5\text{x}10^{18}/\text{cm}^3$ and $1.8\text{x}10^{19}/\text{cm}^3$ for (a), (b), (c) and (d) respectively.

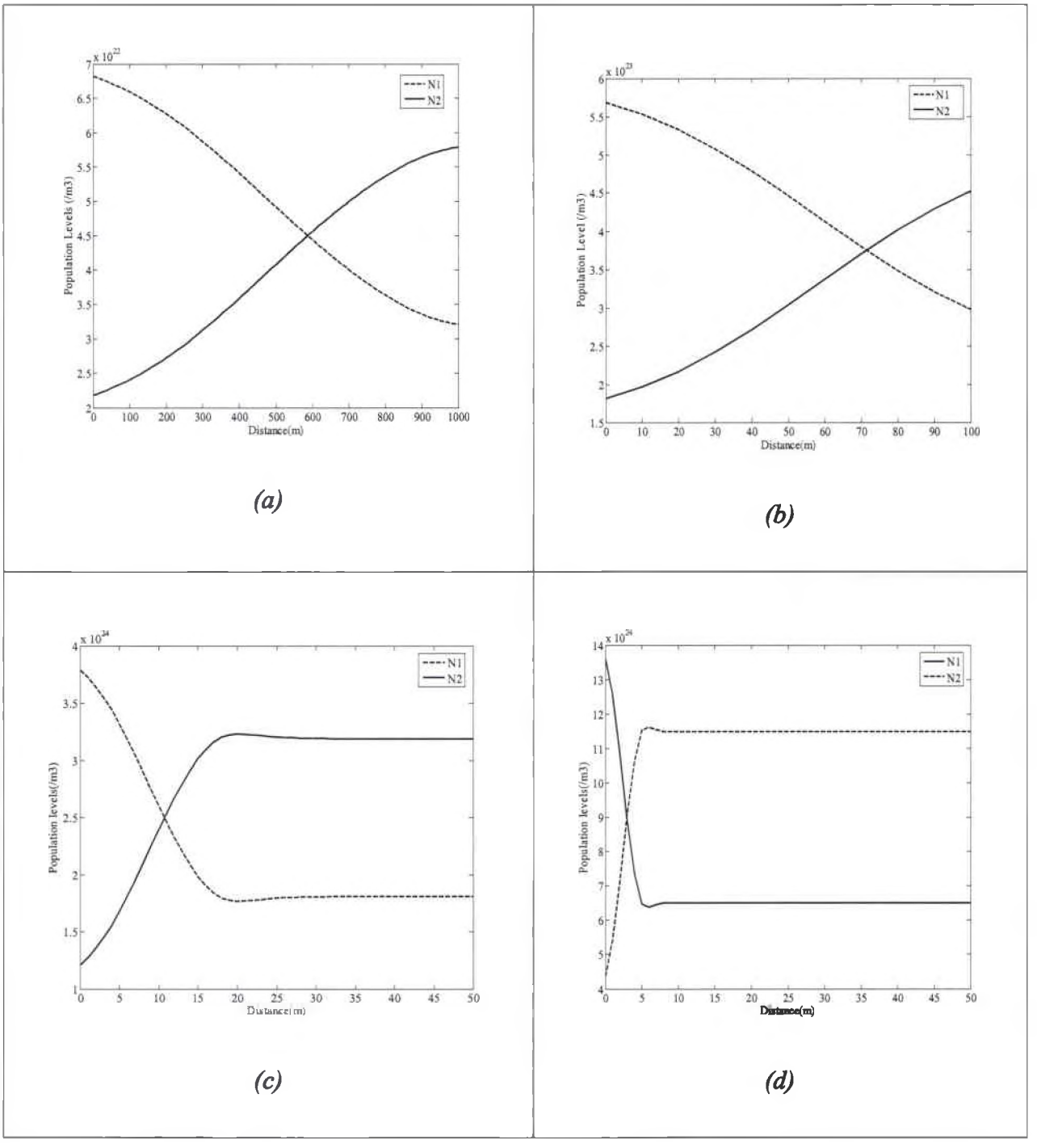

Fig 4.4: Population Inversion for Different Population Densities.

4.5.2 Variation of Input Signal Power

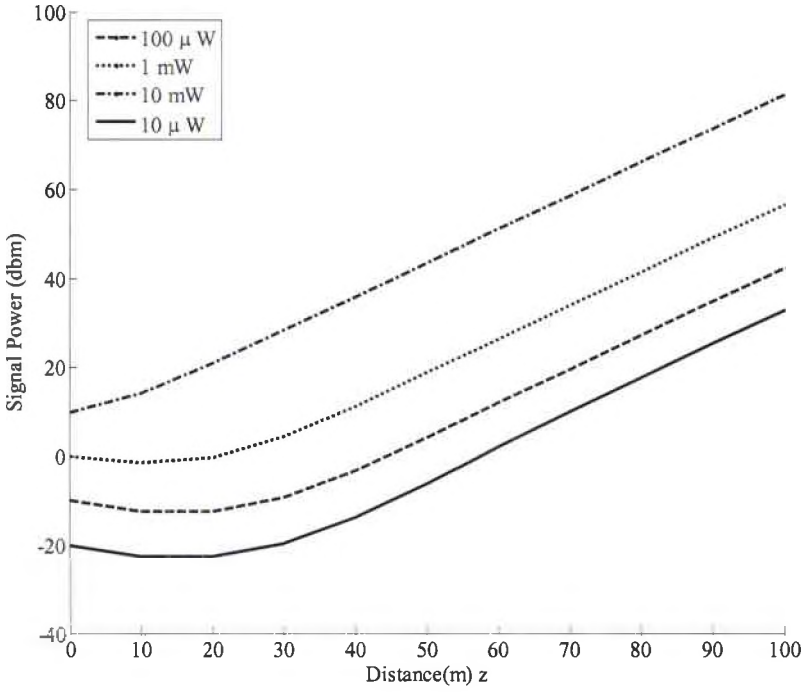

Fig 4.5: Variation of Output Signal Power for Different Input Signal Powers

For a particular length of amplification section the gain is constant. So, as the input signal power is increased the output signal power must increase in order to keep the gain constant. Fig 4.5 shows that signal variation with different input signal powers for a population density N_t = $2x10^{18}/cm^3$, initial pump power of 30mW, pump wavelength $\lambda_p = 1480nm$ and signal wavelength $\lambda_s = 1545nm$.

From Fig 4.7 we can note that for higher input signal powers the decay in the pump power is less. This is also evident from eq. 4.8 which is a pump power variation along the propagation distance, depends upon the input signal power.

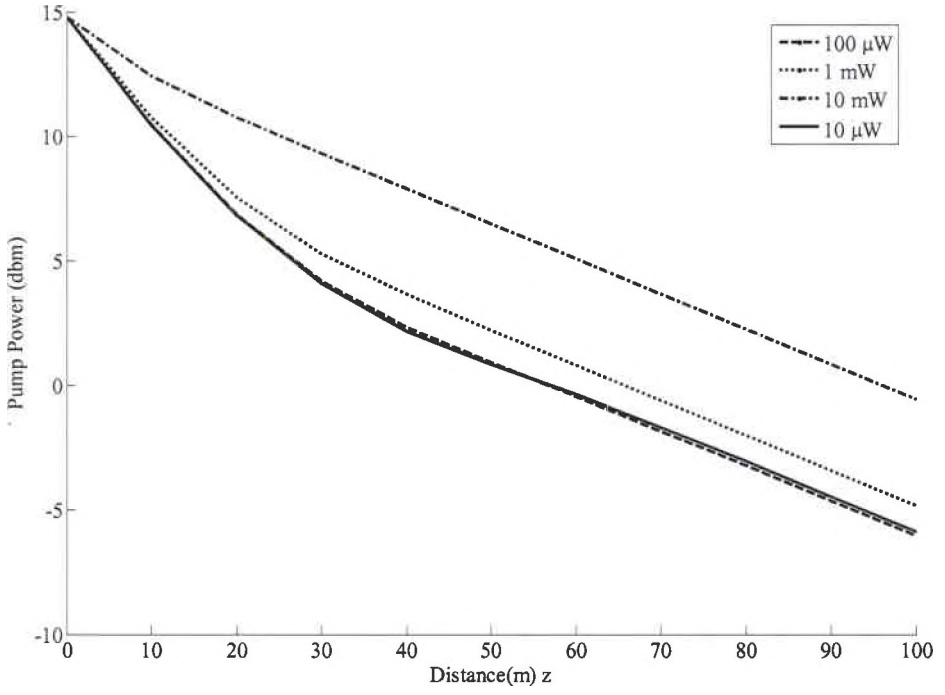

Fig 4.7: Variation of Pump Power for Different Input Signal Powers

It can be noticed from Fig 4.5 that rate of increase in the output signal power is not dependent on the input signal power after a certain distance. The change in the output signal power is given by the eq.(4.9) where the term $\Gamma_s(\sigma_{se}N_2 - \sigma_{sa}N_1)$ determines the rate of change in the output power. The parameters Γ_s, σ_{se} and σ_{sa} are constant values. The variation in the output signal power comes only from the variation in the population densities along the distance. But after a certain distance after the population inversion started, the population levels in the ground and metastable regions stabilize to $1.28\text{x}10^{24}/\text{m}^3$ and $7.2\text{x}10^{23}/\text{m}^3$ irrespective of the input signal power. This is proved in the Fig 4.8(a) and (b). From this point the term $\Gamma_s(\sigma_{se}N_2 - \sigma_{sa}N_1)$ has the same value irrespective of the input signal power which explains the reason for the same slope for all the curves in Fig 4.5. A similar kind of explanation can be given to for the Fig 4.7 which relates to the eq. (4.10).

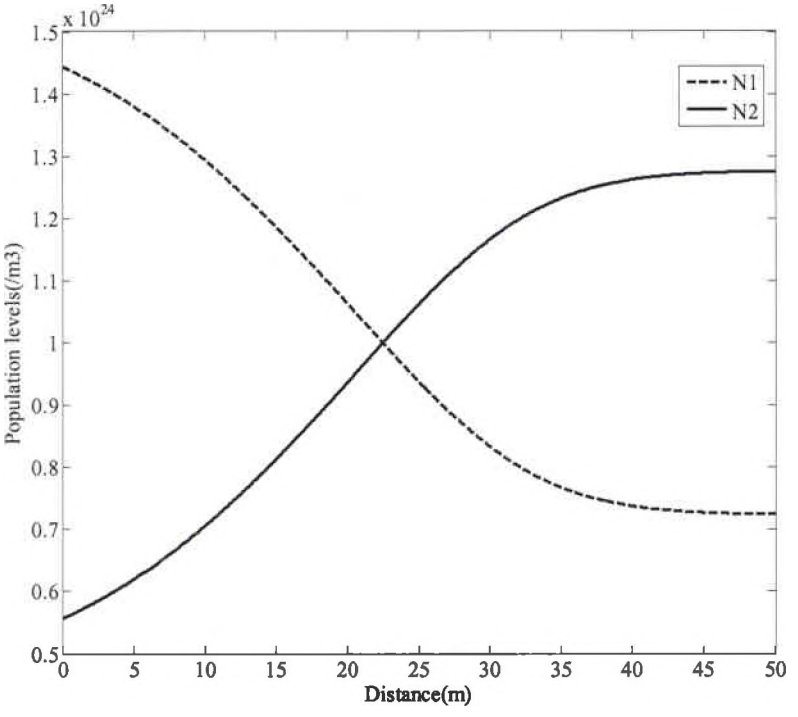

Fig 4.8(a): Population Inversion for Input Signal Power 1mW.

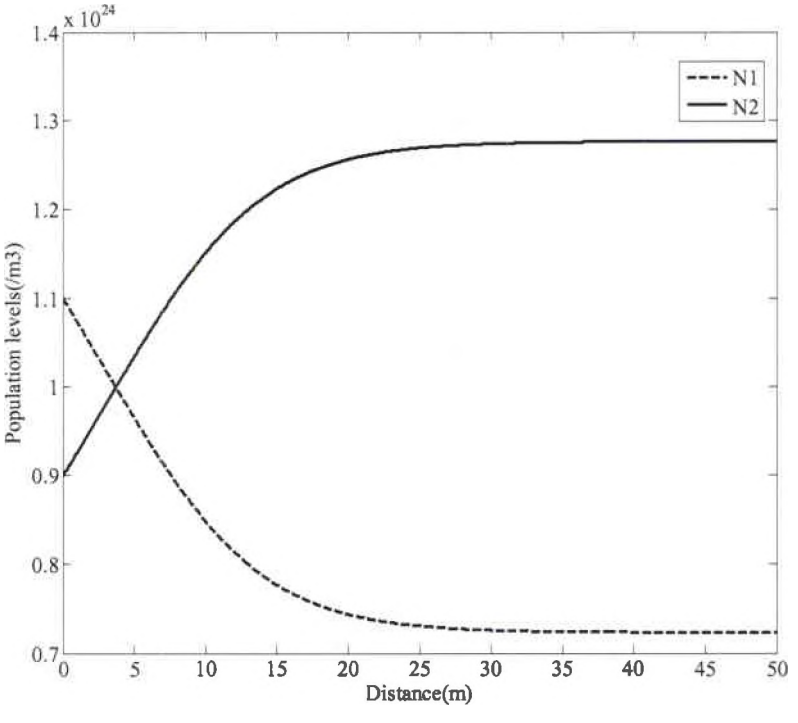

Fig 4.8(b): Population Inversion for Input Signal Power 10mW

4.5.3 Variation of Input Pump Power

In this section the effect of the input pump on the population inversion is observed. In the standard case the pump is taken as 30mW. The effect of the input pump on the population inversion is observed by taking the input pump as 10mW and 50mW. As the input pump is increased the population inversion occurred at a nearer distance. This effect is shown in the Fig 4.9(a) and Fig4.9(b) where the population inversion occurred at 32m and 15m for 10mW and 50mW respectively.

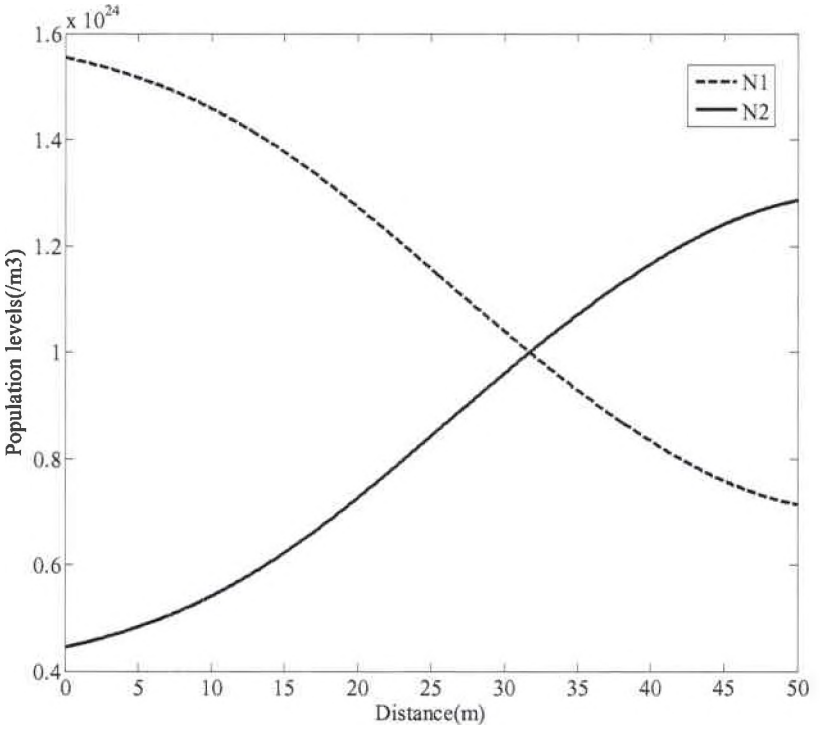

Fig 4.9(a): Population Inversion for Input Pump Power 10mW.

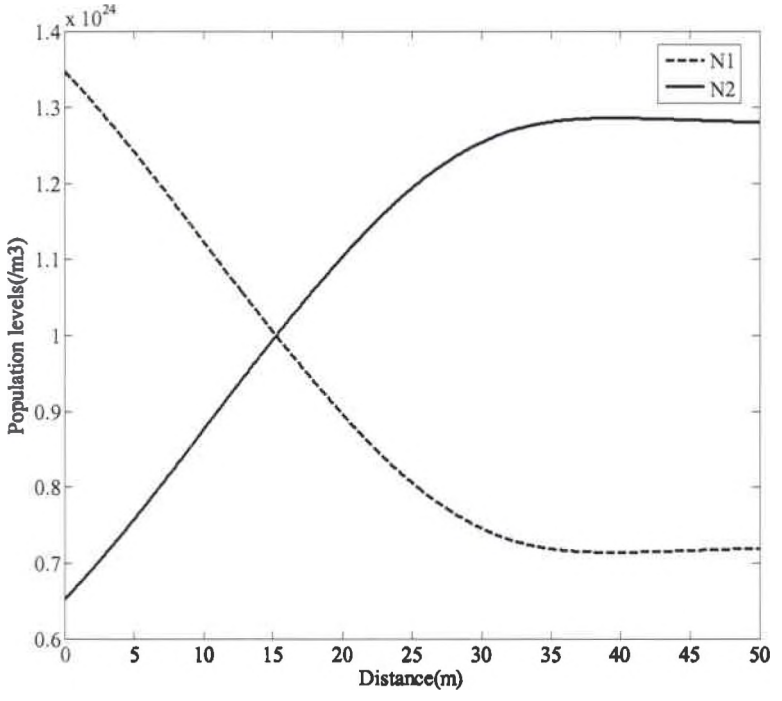

Fig 4.9(b): Population Inversion for Input Pump Power 50mW.

4.5.4 Variation of Pump and Signal Wavelength

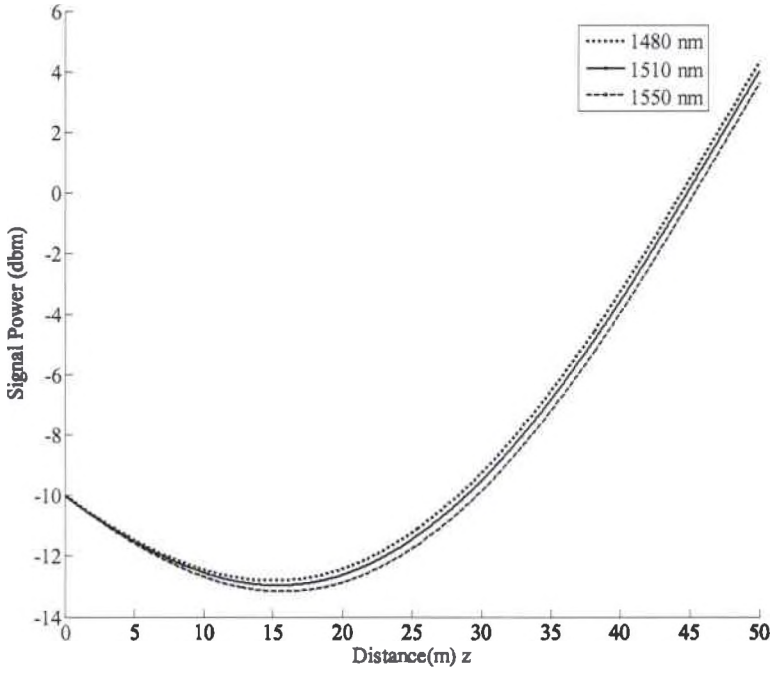

Fig 4.10(a): Variation of Output Signal Power for Different Pump Wavelengths

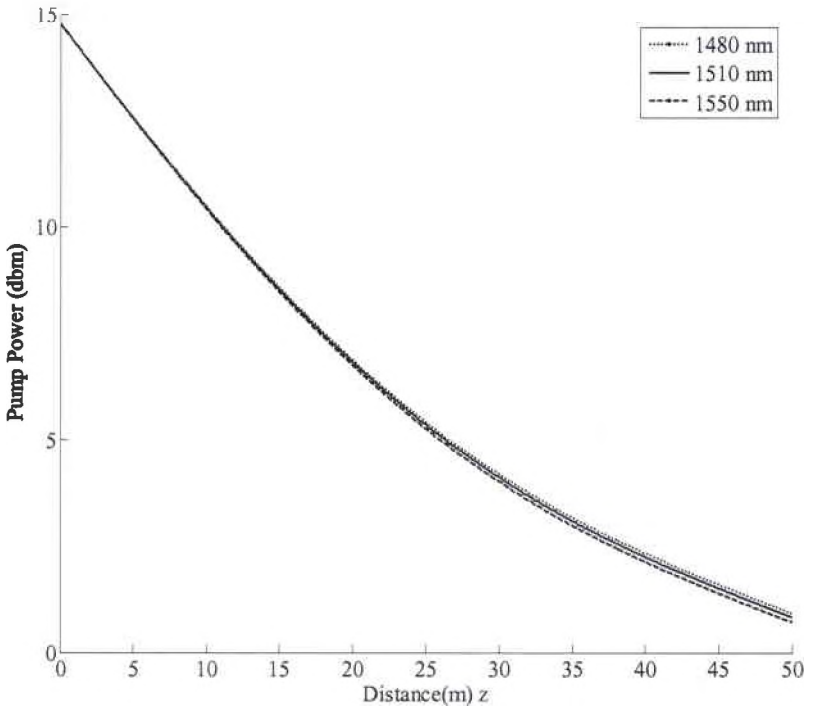

Fig 4.10(b): Variation of Pump Power for Different Pump Wavelengths

Fig 4.10(a) and (b) show the variation of signal and pump power for different pump wavelengths for a population density N_t = $2x10^{18}/cm^3$, signal wavelength $\lambda_s = 1545nm$, initial pump power of 30mW and input signal power of 100μW. Higher the wavelength (lower frequency) energy in the pump is less. This leads to the following result. As the pump wavelength increases the amplification of the signal is less and the decay in the pump power is more. The same thing happens with the variation in signal wavelength. This is shown in Fig 4.11(a) and (b).

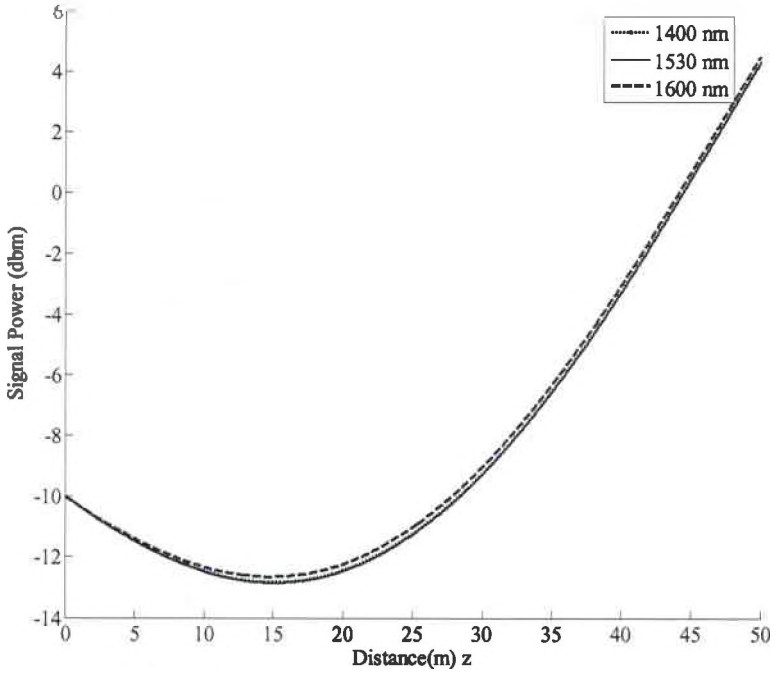

Fig 4.11(a): Variation of Output Signal Power for Different Signal Wavelengths

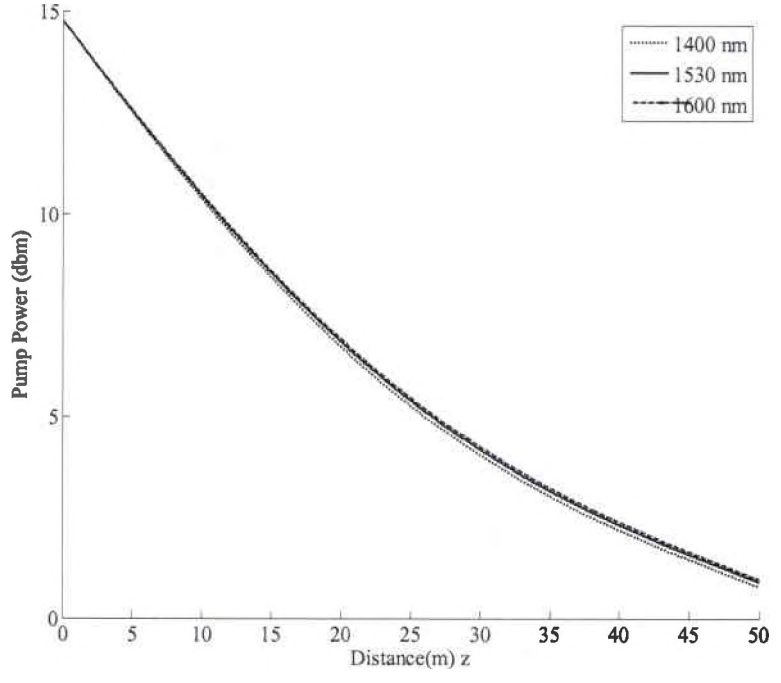

Fig 4.11(b): Variation of Pump Power for Different Signal Wavelengths

4.5.4.1 Effect of Pump and Signal Wavelength on Population Inversion

Variation of the pump wavelength did not shift the position of the population inversion proportionately in the amplifier. This is shown in the series of the plots as Fig 4.12(a), (b), (c) where the pump wavelength is assumed as 1480nm, 1510nm, 1550nm.

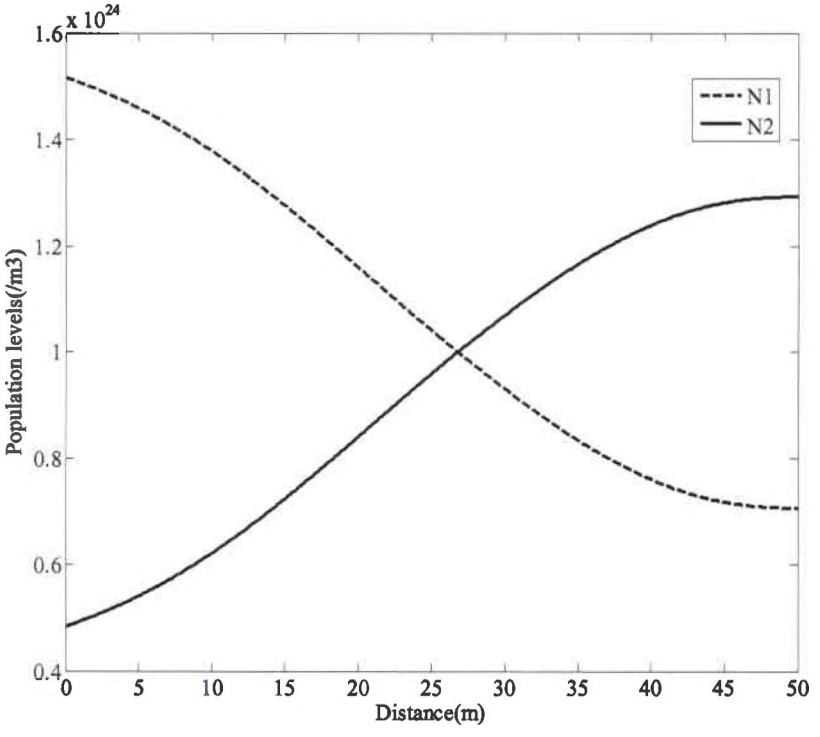

Fig 4.12(a): Population Inversion for Pump Wavelength 1480nm.

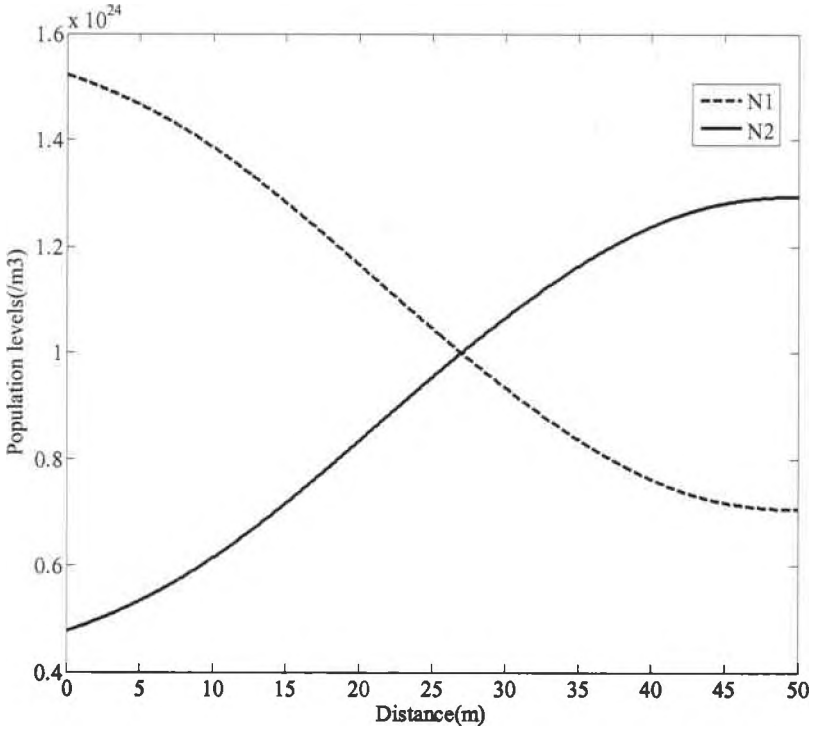

Fig 4.12(b): Population Inversion for Pump Wavelength 1510nm.

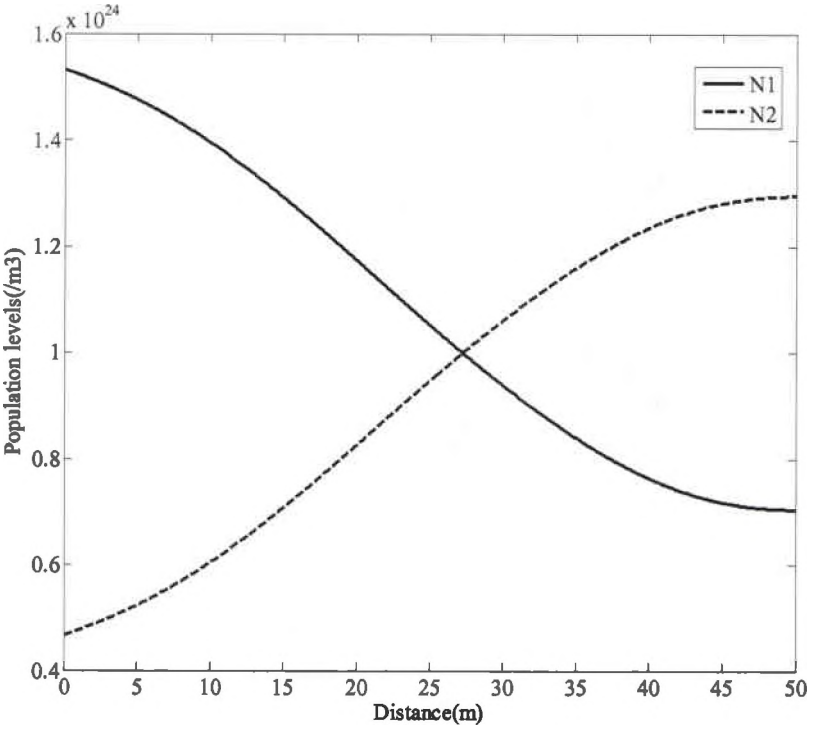

Fig 4.12(c): Population Inversion for Pump Wavelength 1550nm.

It is also observed that the change in the signal wavelength also did not affect the population inversion occurrence. This observation is evident from the plots in Fig 4.13(a), (b) and (c) as the inversion occurred around 26m approximately for all wavelengths used.

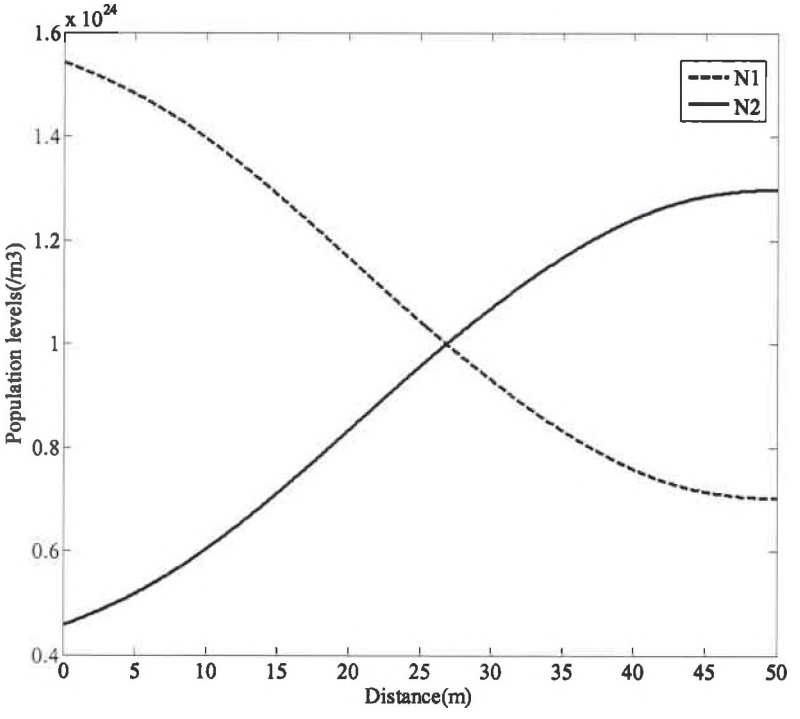

Fig 4.13(a): Population Inversion for Signal Wavelength 1400nm.

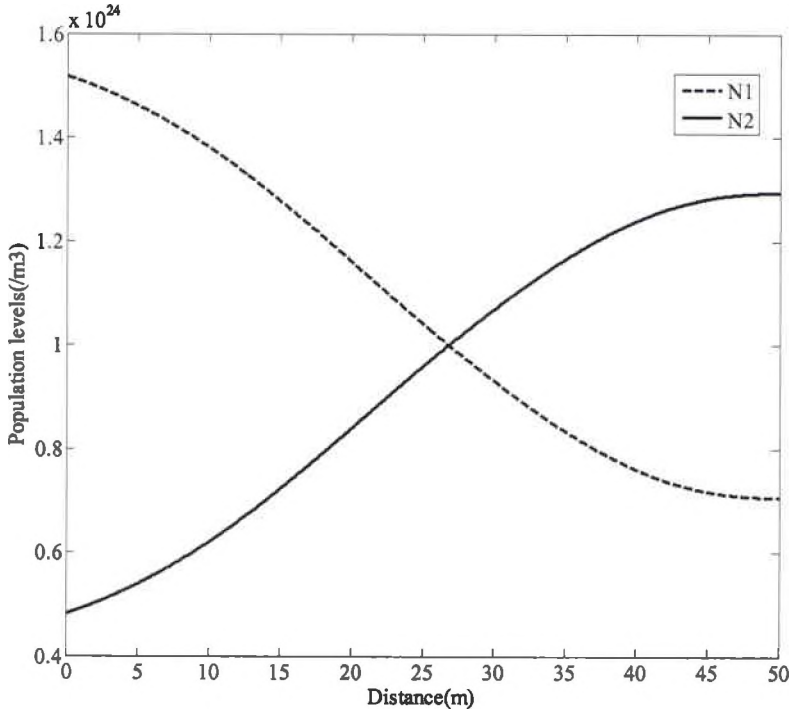

Fig 4.13(b): Population Inversion for Signal Wavelength 1530nm.

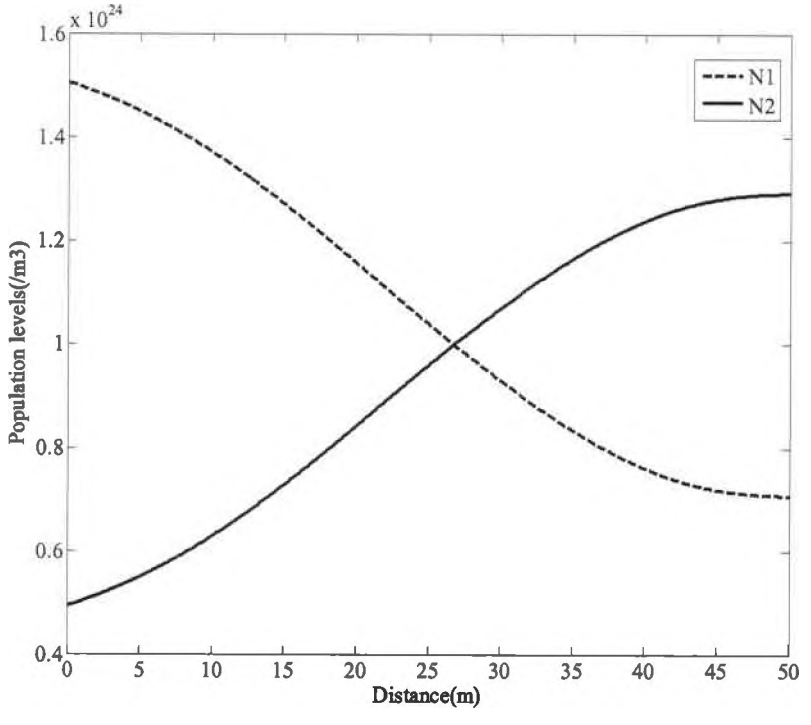

Fig 4.13(c): Population Inversion for Signal Wavelength 1600nm.

4.6 Optimum Parameter Values

The parameters that we could vary during the computations were the input pump power, input signal power, pump wavelength, signal wavelength and the initial population density of the erbium doping. Our goal is to achieve the population inversion in the least distance possible. For this, we have varied all the above mentioned parameters and noticed that enhanced energy transfer effectively results from the variation of the input pump power and the erbium doping as compared to the variation of signal and pump wavelengths in the previous sections. The increase in the input signal strength also shifted the point of population inversion to a closer point. This is explicit as the increase in signal strength would increase the gain and hence the variation in this parameter is not considered for optimization. As the pump power increased the population inversion occurred at a closer point. The same effect is seen for the variation of the erbium doping which is the total population density. So keeping all the other parameter values at the regular values as shown in the Table 4.1 we have varied the pump power and the population density. We have considered the population density $N_t = 5\times10^{18}$ and the input pump power as 50mW for one case. At these values the population inversion occurred at around 6.1m as shown in Fig 4.14. In the second case we have further increased the erbium doping to $N_t = 8\times10^{18}$ keeping the pump power at 50mW. Under these conditions the population inversion moved much closer and occurred at around 3.8m as shown in Fig 4.15.

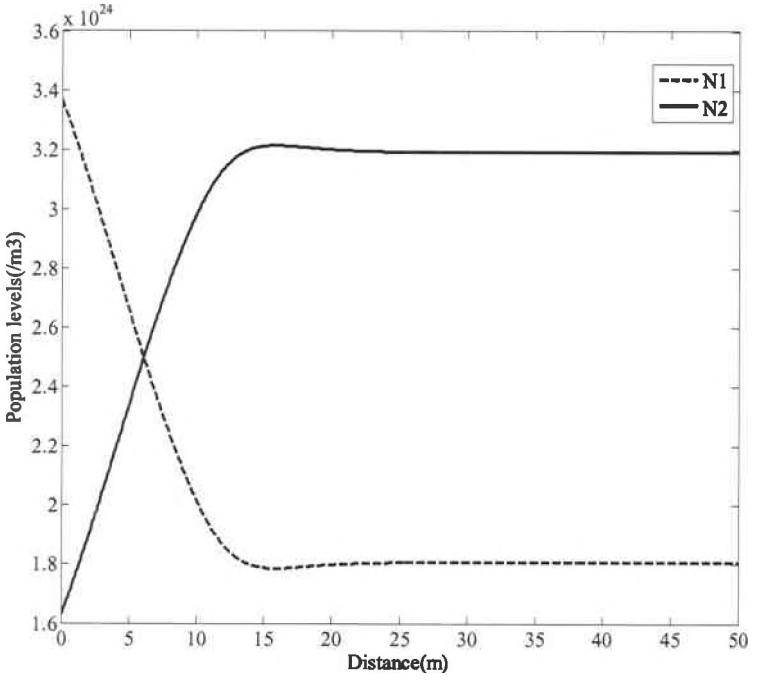

Fig 4.14: Population Inversion for $N_t = 5\times10^{18}$, Input Pump Power 50mW, Input Signal Power 100 μW.

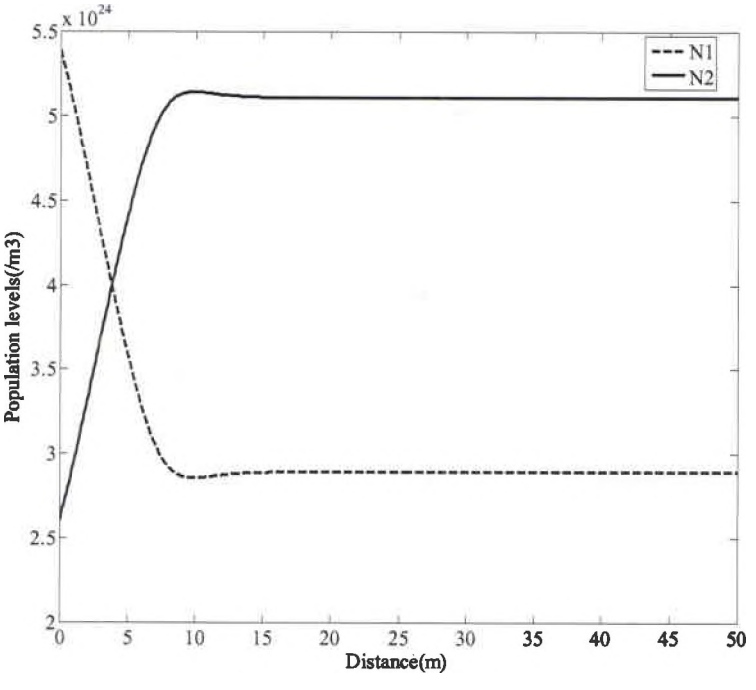

Fig 4.15: Population Inversion for $N_t = 8\times10^{18}$, Input Pump Power 50mW and Input Signal Power 100 μW.

4.7 Accuracy of the Analysis and Plots

The accuracy of the whole analysis is verified by checking the values of the pump and signal power for various propagation step size. The pump and signal powers at 30m form the start of the EDFA section for different propagation step sizes is tabulated in table 4.3. For larger propagation steps the power values vary drastically indicating the high error rate. But as the step size reduces pump and signal powers values converged to an accurate value. This convergence shows that for values less than step size of .1m our analysis is valid.

Table 4.2 Pump and Signal Powers for different Δz at $z = 30m$

Δz(m)	Pump Power	Signal Power
10	5.6817	-10.6958
5	4.9283	-10.0139
2	4.5434	-9.5926
1	4.2499	-9.2821
0.5	4.1865	-9.2204
0.2	4.1801	-9.2197
0.1	4.1759	-9.2047
0.05	4.1746	-9.2038
0.02	4.1734	-9.2023
0.01	4.1731	-9.2019

4.8 Solution for the EDFA Power Evolution Equations - Analytical Representation

The analytical solution of the Desurvire Equations is given below. Signal and ASE grow along the fiber length and pump power decays exponentially as it travels along the fiber. The initial ASE $P_a(0)$ is not equal to zero. It is assumed to be 10^{-12} Watts.

$$P_p(z) = P_p(0)\exp(-A_1 z)$$

$$P_s(z) = P_s(0)\exp(A_2 z)$$

$$P_a(z) = \exp(A_3(z + \frac{\ln(A_4 / A_3)}{A_3}))$$

$$A_1 = [(\sigma_{pa}N_1 - \sigma_{pe}N_2)\Gamma_p + \alpha_p]$$

$$A_2 = A_3 = [(\sigma_{se}N_2 - \sigma_{sa}N_1)\Gamma_s - \alpha_s]$$

$$A_4 = 2\sigma_{se}N_2 h\upsilon_s\Gamma_s\Delta\upsilon$$

4.8 Conclusion

Franco neglected attenuation in the transmission fiber. Moreover, Franco's equations are power spectral density equations and Desurvire's equations are power equations. The detailed analysis in this chapter shows that, in the case of pure numerical solutions, the ASE and signal power increase along the length of the EDFA section. But taking a closer look on the signal power more realistic pump power fitting will lead to accurate signal power evolution. The set of eqs. (3.1), (3.2) and (3.3) when compared with the (4.8), (4.9) and (4.10) eqs. respectively look structurally symmetric.

CHAPTER 5

SUMMARY AND CONCLUSIONS

5.1 Summary:

To overcome the problem of signal attenuation during long distance propogation, electronic regenerators limited by the speed of the electronic components have been used for many years. With the advent of fiber optic communications, electronic regenerators are being replaced by optical amplifiers based on the phenomenon of stimulated emission. Optical amplifiers serve fiber communication systems in several ways. Since the 80s, many researchers and scientists throughout the world have worked to improve amplifiers so as to increase their bandwidth and channel capacity.

SLAs, Raman amplifiers, Brillouin amplifiers and rare earth ion doped fiber amplifiers are different types of fiber amplifiers that have been used for amplification purposes [23]. Certain characteristics such as gain saturation, ASE power, noise figure and signal gain define an optical amplifier. In-line amplifiers, power amplifiers, LAN amplifiers are some examples of the applications of optical amplifiers. Of the different kinds of optical amplifiers we have analyzed the erbium doped fiber amplifiers (EDFAs) because they have better cross-talk characteristics, higher operating power, lower insertion loss, broader bandwidth, higher efficiency and low noise figure. In addition,

they can be used both as distributed and lumped amplifiers. The architecture, characteristics and the spectrum of erbium dopant are also discussed.

The three level laser system model [24] for the evolution of signal and ASE power due to an applied pump power is found to be an easy and efficient way of analyzing the EDFA section in fiber communications. We have analyzed the evolution equations for signal and ASE power densities using the numerical method given in chapter 4. This method is found to be so much at bit tedious, but accurate. The growth of the population densities of both ground and metastable levels is numerically solved under temporal steady state in the direction of propagation. The resulting population densities illustrate the occurrence of population inversion at a cross over point which leads to the amplification in EDFAs. The evolution equations which are solved numerically, are also plotted by varying parameters such as initial pump and input signal powers, the level of erbium doping, and pump and signal wavelengths within the optimum range. The effects of these parameters on the behavior of the EDFA have been analyzed. Based on these results, an optimum set of values has been suggested for the parameters in order to obtain the population inversion in the shortest possible distance (approximately less than 10m). Further we used quasi analytical solution fitting for the rate equations as suggested by P. Franco [22] and a more exact result solved from a modified set of equations. The trends in the plots generated using the solution appear to match with the numerical solution suggested by E. Desurvire [20].

5.2 Future Work:

We have solved the spatial evolution equation for the EDFA section for temporal steady state conditions. If we consider non steady state in both space and time we obtain

highly nonlinear coupled differential equations; ideally, solutions to such equations would provide better insight into the transient dynamics of population and power. This may be pursued as an extension of this work. Moreover, in the quasi analytical solution for the rate equation suggested in chapter 3 consist of only few parameters. We can add more parameters such as the attenuation losses of signal and power in the fiber to the power equation solution fitting, which will yield a precise result. Before making a fitting we should compare and analyze the solution between the two methods suggested in chapters 3 and 4. This will allow us to choose an optimum set of parameters, so that the computation does not become large, and the result obtained is precise with in an error margin.

Bibliography

1. J. E. Geusic and H. E. D. Scovil, "A unidirectional traveling-wave optical laser," *Bell Syst. Tech. J.* **41,** 1371 (1962).

2. E. Snitzer and R. Woodcock, "Yb3+-Er3+ glass laser," *Appl. Phys. Lett.* **6**, 45 (1965).

3. J. Stone and C. A. Burrus, "Neodymium-doped silica lasers in end-pumped fiber geometry," *Appl. Phys. Lett.* **23**, 388 (1973).

4. R. J. Mears, L. Reekie, I. M. Jaunice, and D. N. Payne, "High-gain rare-earth doped fiber amplifier at 1.54 μm," *Optical Fiber Communication Conference.* **3**, 167 (1987)

5. E. Snitzer, H. Po, F. Hakimi, R. Tuminelli, and B. C. MaCollum, "Erbium fiber laser amplifier at 1.55 μm with pump at 1.49 μm and Yb sensitized Er oscillator," *Optical Fiber Communication Conference.* **1,** 218 (1988).

6. M. Nakazawa, K. Suzuki, and Y. Kimura, "Efficient Er^{3+} - doped optical fiber amplifier pumped by a 1.48 μm InGaAsP laser diode," *Appl. Phys. Lett.* **54**, 295 (1989).

7. N. A. Olsson, *J. Light. Tech.* **7**, 1071 (1989).

8. N. Edagawa, K. Mochizuki, and H. Wakabayashi, "1.2Gbit/s, 218 km Transmission Experiment Using Inline Er-Doped Fibre Amplifier," *Elect. Lett.* **25,** 363 (1989).

9. S. B. Poole, D. N. Payne, and M. E. Fermann, "Fabrication of low loss optical fibers containing rare-earth ions," *Elect. Lett.* **21,** 737 (1985).

10. L. Reekie, R. J. Mears, S. B. Poole and D. N. Payne, "Tunable single-mode fiber lasers," *J. Light. Tech.* **4**, 956 (1986).

11. R. J. Mears *et.al.,* "High-gain rare-earth doped fiber amplifier at 1.54 μm," *Optical Fiber Communication Conference.* **12,** 19 (1987).

12. C. A. Millar, "Thermal properties of an erbium-doped fiber amplifier," *Elect. Lett.* **23,** 865 (1987).

13. L. Reekie, I. M. Jauncey, S. B. Poole, and D. N. Payne, "Diode Laser pumped operation of an Er^{3+} doped single mode fiber laser," *Elect. Lett.* **23,** 1076 (1987).

14. R. I. Laming, S. B. Poole, and E. J. Tarbox, "Pump excited-state absorption in erbium-doped fibers," *Opt. Lett.* **13,** 1084 (1988).

15. E. Desurvire *et.al.,* "2-Gbit/s signal amplification at λ=1.53 μm in an erbium-doped single-mode fiber amplifier," *Opt. Lett.* **14,** 1266 (1989).

16. Y. Kimura, K. Suzuki, and M. Nakazawa, "Soliton amplification and transmission with Er^{3+}-dopedfibre repeater pumped by GaInAsP diode," *Elect. Lett.* **25,** 1656 (1989).

17. E. Desurvire, C. R. Giles, and J. R. Simpson, "Saturation-induced crosstalk in high speed erbium doped fiber amplifiers at I = 1.53 μm," *Optical Fiber Communication Conference.* **7**, 14 (1989).

18. R. E. Wagner *et.al.,* "16-channel coherent broadcast network at 155 Mb/s," *Optical Fiber Communication Conference.* **12**, 21 (1989).

19. H. Taga *et.al.,* "459 km, 2.4 Gbit/s 4 wavelength multiplexing optical fiber transmission experiment using 6 Er-doped fiber amplifiers," *Optical Fiber Communication Conference.* **9**, 23 (1990).

20. C. R. Giles and E. Desurvire, "Propagation of Signal and Noise in Concatenated Erbium Doped Fiber Optical Amplifiers," *J. Light. Tech* **9**, 147 (1991).

21. E. Desurvire and J. R. Simpson, "Amplification of Spontaneous Emission in Erbium-Doped Single-Mode Fibers," *J. Light. Tech.* **7**, 835 (1989).

22. Pierluigi Franco and Michele Midrio, "Quasi-analytic solution of erbium-doped fiber-amplifier power equations," *Appl. Opt.* **32,** 7442 (1993).

23. G. P. Agrawal, *Fiber- Optic Communication Systems.* New York: John Wiley & Sons, 1992.

24. P. C. Becker, N. A. Olsson and J. R. Simpson, *Erbium Doped Fiber Amplifiers: Fundamentals and Technology.* San Diego: Academic Press, 1999.

25. J. Hecht, "The Evolution of Optical Amplifiers," *Optical and Photonics News* **13,** 36 (2002).

26. Hansel E. Lee Jr., "A research paper on Erbium Doped fiber Amplifiers," *Optical Comm. Systems,* (1996). Available at http://hansel.hansel.com/papers/erbium.html

27. E. Desurvire, *Erbium Doped Fiber Amplifiers: Principles and* Applications. New York: John Wiley & Sons, 1987

28. E. Desurvire, J. R. Simpson, and P. C. Becker, "High-gain erbium-doped traveling-wave fiber amplifier," *Opt. Lett.* **12,** 888 (1987).

29. K. Nakagawa, S. Nishi, K. Aida, and E. Yoneda, "Trunk and distribution network application of erbium-doped fiber amplifier," *J. Light. Tech.* **9,** 198 (1991)

30. Mukai, T., K. Inoue and T. Saito, "Homogeneous gain saturation in 1.5mm InGaAsP traveling wave semiconductor laser amplifiers," *Appl. Phys. Lett.* **51**, 366 (1987).

31. M. J. F. Digonnet, *Rare Earth Doped Fiber Lasers and Amplifiers*. New York: Marcel Dekker Inc, 1993.

32. R. H. Stolen, E. P. Ippen, and A.R. Tynes, "Raman oscillation in glass Optical waveguides," *Appl. Phys. Lett.* **20**, 62 (1972);
R. H. Stolen and E. P. Ippen, "Raman gain in glass optical waveguides," *Appl. Phys. Lett.* **22**, 276 (1973).

33. N. Edagawa, K. Mochizuki, S. Ryu and H. Wakabayashi, "Amplification characteristics of fiber Raman Amplifiers," *ICICE Technical Report.* **88,** 33 (1988).

34. C. G. Atkins, D. Cotter, D.W. Smith and R. Wyatt, "Application of Brillouin amplification in coherent optical transmission," *Elect. Lett.* **22**, 348 (1986).

35. R. J. Mears, L. Reekie, I. M. Jauncey, and D. N. Payne, "Low-Noise Erbium-Doped Fiber Amplifier Operating at 1.54μm," *Elect. Lett.* **23**, 1026 (1987).

36. B. E. A. Saleh and M. C. Teich, *Fundamentals of Photonics,* New York: John Wiley & Sons, 1991.

37. C. Bendjaballah and M. Charbit, "Detection of optical signals in generalized Gaussian noise," *IEEE Trans. Comm.* **73**, 1840 (1983).

38. M. J. F. Digonnet, "Closed-form expressions for the gain in three- and four-level laser fibers," *IEEE J. Quant. Elect.* **26**, 1788 (1990).

39. Y. Ohishi, T. Kanamori, T. Kitagawa, S. Takahashi, E. Snitzer and G. H. Sigel, "Pr^{3+} doped fluoride fiber amplifier operating at 1.31μm," *Optical Fiber Communication Conference.* **4**, 237 (1991).

40. M. Shimizu, T. Kanamori, J. Temmyo, M. Wada, M. Yamada, Y. Terunuma, Y. Ohishi and S. Sudo, "28.3 dB gain 1.3μm band Pr-doped fluoride fiber amplifier module pumped by 1.017μm InGaAs – LD's," *IEEE Phot. Tech. Lett.* **5**, 654 (1993).
41. M. Yamada, M. Shimizu, T. Kanamori, Y. Ohishi, Y. Terunuma, K. Oikawa, H. Yoshinaga, K. Kikushima, Y. Miyamoto, and S. Sudo, "Low-noise and high – power Pr^{3+} -doped fluoride fiber amplifier," *IEEE Phot. Tech. Lett.* **7**, 869 (1995).

42. S. Sanders, K. Dzurko, R. Parke, S. O'Brien, D. F. Welch, S. G. Grubb, G. Nykolak, and P. C. Becker, "Praseodymium doped fibre amplifiers (PDFAs) pumped by monolithic master oscillator power amplifier (M-MOPA) laser diodes," *Elect. Lett.* **32**, 343 (1993).

43. M. L. Dakss and W. J. Miniscalco, "A large-signal model and signal/noise ratio analysis for Nd^{3+} doped fiber amplifiers at 1.3μm," *Fiber Laser Sources and Amplifiers II.* **1373,** 111 (1990).

44. W. J. Miniscalco, L. J. Andrews, B. A. Thompson, R. S. Quimbly, L. J. B. Vacha, and M. G. Drexhage, "1.3 μm fluoride fibre laser," *Elect. Lett.* **24**, 28 (1988).

45. M. Brierley, S. Carter, P. France, and J. E. Pederson, "Amplification in the 1300 nm telecommunications window in an Nd-doped fluoride fiber," *Elect. Lett.* **26**, 330 (1990).

46. Y. Miyajima, T. Sugawa, and T. Komukai, "10 dB gain and high saturation in a Nd^{3+} - doped fluorozirconate fiber amplifier," *Elect. Lett.* **26**, 1398 (1990).

47. E. Ishikawa, H. Aoki, T. Yamashita, and Y. Asahara, "Laser emission and amplification at 1.3μm in neodymium – doped fluorophosphates fibres," *Elect. Lett.* **28**, 1497 (1992).

48. Vivek Mehta., Amplified Spontaneous Emission available at http://light.utoronto.ca/vmehta/ase.pdf